



Search for supersymmetry in the vector-boson fusion topology in proton-proton collisions at $\sqrt{s} = 8$ TeV

The CMS Collaboration*

Abstract

The first search for supersymmetry in the vector-boson fusion topology is presented. The search targets final states with at least two leptons, large missing transverse momentum, and two jets with a large separation in rapidity. The data sample corresponds to an integrated luminosity of 19.7 fb^{-1} of proton-proton collisions at $\sqrt{s} = 8$ TeV collected with the CMS detector at the CERN LHC. The observed dijet invariant mass spectrum is found to be consistent with the expected standard model prediction. Upper limits are set on the cross sections for chargino and neutralino production with two associated jets, assuming the supersymmetric partner of the τ lepton to be the lightest slepton and the lightest slepton to be lighter than the charginos. For a so-called compressed-mass-spectrum scenario in which the mass difference between the lightest supersymmetric particle $\tilde{\chi}_1^0$ and the next lightest, mass-degenerate, gaugino particles $\tilde{\chi}_2^0$ and $\tilde{\chi}_1^\pm$ is 50 GeV, a mass lower limit of 170 GeV is set for these latter two particles.

Published in the Journal of High Energy Physics as doi:10.1007/JHEP11(2015)189.

1 Introduction

With the successful operation of the CERN LHC, numerous results placing constraints on extensions to the standard model (SM) have been presented by the ATLAS and CMS experiments. In particular, in models of supersymmetry (SUSY) [1–7], limits in excess of 1 TeV have been placed on the masses of the strongly produced gluinos and first- and second-generation squarks [8–15]. In contrast, mass limits on the weakly produced charginos ($\tilde{\chi}_i^\pm$) and neutralinos ($\tilde{\chi}_i^0$), with much smaller production cross sections, are much less severe. The limits for charginos and neutralinos are especially weak in so-called compressed-mass-spectrum scenarios, in which the mass of the lightest supersymmetric particle (LSP) is only slightly less than the masses of other SUSY states. The chargino-neutralino sector plays a crucial role in the connection between dark matter and SUSY: in SUSY models with R-parity [16] conservation, the lightest neutralino $\tilde{\chi}_1^0$ often takes the role of the LSP and is a dark matter candidate.

Previous LHC searches [17, 18] for electroweak chargino and neutralino production have focused on final states with one or more leptons (ℓ) and missing transverse momentum (\vec{p}_T^{miss}), e.g., $\tilde{\chi}_1^\pm \tilde{\chi}_2^0$ pair production followed by $\tilde{\chi}_1^\pm \rightarrow \ell \nu \tilde{\chi}_1^0$ and $\tilde{\chi}_2^0 \rightarrow \ell \ell \tilde{\chi}_1^0$, where $\tilde{\chi}_1^\pm$ ($\tilde{\chi}_2^0$) is the lightest (next-to-lightest) chargino (neutralino), and where the LSP $\tilde{\chi}_1^0$ is presumed to escape without detection leading to significant p_T^{miss} . However, these searches exhibit limited sensitivity in cases where the $\tilde{\chi}_1^\pm$ and $\tilde{\chi}_2^0$ are nearly mass degenerate with the $\tilde{\chi}_1^0$. The mass difference $\Delta m = m_{\tilde{\chi}_1^\pm} - m_{\tilde{\chi}_1^0}$ is a crucial parameter dictating the sensitivity of the analysis. While the exclusion limits in Refs. [17, 18] can be as large as $m_{\tilde{\chi}_1^\pm} < 720$ GeV for a massless $\tilde{\chi}_1^0$, they weaken to only ≈ 100 GeV for $\Delta m < 50$ GeV. The current searches also exhibit limited sensitivity to models with SUSY particles that decay predominantly to τ leptons, even for LSP masses near zero, due to the larger backgrounds associated with τ -lepton reconstruction compared to electrons or muons.

Electroweak SUSY particles can be pair produced in association with two jets in pure electroweak processes in the vector-boson fusion (VBF) topology [19], which is characterized by the presence of two forward jets (i.e. jets near the beam axis), in opposite hemispheres, leading to a large dijet invariant mass (m_{jj}). Figure 1 shows the Feynman diagrams for two of the possible VBF production processes: chargino-neutralino and chargino-chargino production.

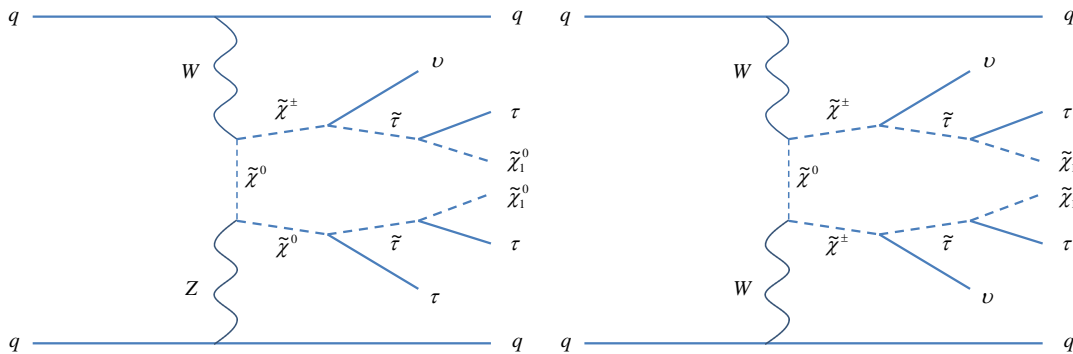


Figure 1: Diagrams of (left) chargino-neutralino and (right) chargino-chargino pair production through vector-boson fusion followed by their decays to leptons and the LSP $\tilde{\chi}_1^0$.

A search in the VBF topology offers a new and complementary means to directly probe the electroweak sector of SUSY, especially in compressed-mass-spectrum scenarios [20]. It targets unexplored regions of SUSY parameter space, where other searches have limited sensitivity.

It differs fundamentally from the conventional direct electroweak SUSY searches mentioned above in that it uses the presence of jets with large transverse momenta (p_T) to suppress SM background. In this regard, it resembles searches for strongly produced SUSY particles. However, unlike these latter studies, which present searches for the indirect production of charginos and neutralinos through squark or gluino decay chains [10–12], the VBF search does not require the production of squarks or gluinos, whose masses might be too large to allow production at the LHC.

In this paper, we present a search for the electroweak production of SUSY particles in the VBF topology. The data, corresponding to an integrated luminosity of 19.7 fb^{-1} of proton-proton collisions at a centre-of-mass energy of $\sqrt{s} = 8 \text{ TeV}$, were collected with the CMS detector in 2012. Besides the two oppositely directed forward jets (j) that define the VBF configuration, the search requires the presence of at least two leptons ($e, \mu, \text{ or } \tau$) and large p_T^{miss} . The events are classified into one of eight final states depending on the dilepton content and charges $e\mu jj$, $\mu\mu jj$, $\mu\tau_h jj$, and $\tau_h\tau_h jj$, where τ_h denotes a hadronically decaying τ lepton and where we differentiate between final states with same-sign (SS) and opposite-sign (OS) dilepton pairs. The dijet invariant mass distribution m_{jj} is used to search for the SUSY signal. Stringent requirements are placed on p_T^{miss} and on the kinematic properties of the VBF dijet system to suppress SM background. In particular, the R-parity conserving SUSY models we examine predict much higher average dijet p_T than is typical for SM processes such as VBF Higgs boson production [21], allowing us to suppress the background by a factor of 10^2 – 10^4 , depending on the background process.

The background is evaluated using data wherever possible. The general strategy is to define control regions, each dominated by a different background process, through modification of the nominal selection requirements. These control regions are used to measure the m_{jj} shapes and probabilities for background events to satisfy the VBF selection requirements. If the background contribution from a particular process is expected to be small or if the above approach is not feasible, the m_{jj} shapes are taken from simulation. In these cases, scale factors, defined as the ratio of efficiencies measured in data and simulation, are used to normalize the predicted rates to the data.

The paper is organized as follows. The CMS detector is described in Section 2. The reconstruction of electrons, muons, τ_h leptons, jets, and p_T^{miss} is presented in Section 3. The dominant backgrounds and their simulated samples are discussed in Section 4, followed by the description of the event selection in Section 5 and the background estimation in Section 6. Systematic uncertainties are summarized in Section 7, and the results are presented in Section 8. Section 9 contains a summary.

2 CMS detector

The central feature of the CMS apparatus is a superconducting solenoid of 6 m internal diameter, providing a magnetic field of 3.8 T. Located within the solenoid volume are a silicon pixel and strip tracker, a lead tungstate electromagnetic calorimeter (ECAL), and a brass and scintillator hadron calorimeter. Muons are measured in gas-ionisation detectors embedded in the steel flux-return yoke outside the solenoid. Extensive forward calorimetry complements the coverage provided by the barrel and endcap detectors. Forward hadron calorimeters on each side of the CMS interaction point cover the very forward angles of CMS, in the pseudorapidity range $3.0 < |\eta| < 5.0$.

The inner tracker measures charged tracks with $|\eta| < 2.5$ and provides an impact paramete-

ter resolution of $\approx 15 \mu\text{m}$ and a transverse momentum resolution of about 1.5% for 100 GeV charged particles. Events are selected with a first-level trigger made of a system of fast electronics, and a high-level trigger that consists of a farm of commercial CPUs running a version of the offline reconstruction optimized for fast processing. A detailed description of the CMS detector, along with a definition of the coordinate system and relevant kinematic variables, can be found in Ref. [22].

3 Object reconstruction and identification

The missing transverse momentum vector \vec{p}_T^{miss} is defined as the projection on the plane perpendicular to the beam axis of the negative vector sum of the momenta of all reconstructed particles in an event. Its magnitude is referred to as p_T^{miss} . The jets and p_T^{miss} are reconstructed with the particle-flow algorithm [23, 24]. The anti- k_T clustering algorithm [25] with a distance parameter of 0.5 is used for jet clustering. Jets are required to satisfy identification criteria designed to reject particles from multiple proton-proton interactions (pileup) and anomalous behavior from the calorimeters. For jets with $p_T > 30 \text{ GeV}$ and $|\eta| < 2.5$ ($2.5 < |\eta| < 5.0$), the reconstruction-plus-identification efficiency is $\approx 99\%$ (95%), while 90–95% (60%) of pileup jets are rejected [26]. The jet energy scale and resolution are calibrated through correction factors that depend on the p_T and η of the jet [27]. Jets originating from the hadronisation of bottom quarks (b quark jets) are identified using the loose working point of the combined secondary vertex (CSV) algorithm [28], which exploits observables related to the long lifetime of b hadrons. For jets with $p_T > 20 \text{ GeV}$ and $|\eta| < 2.4$, the probability of correctly identifying a b quark jet is $\approx 85\%$, while the probability of misidentifying a jet originating from a light quark or gluon as a b quark jet is $\approx 10\%$ [29].

Muons are reconstructed [30] using the inner silicon tracker and muon detectors. Quality requirements based on the minimum number of hits in the silicon tracker, pixel detector, and muon detectors are applied to suppress backgrounds from decays-in-flight and hadron shower remnants that reach the muon system. Electrons are reconstructed [31] by combining tracks produced by the Gaussian-sum filter algorithm with ECAL clusters. Requirements on the track quality, the shape of the energy deposits in the ECAL, and the compatibility of the measurements from the tracker and the ECAL are imposed to distinguish prompt electrons from charged pions and from electrons produced by photon conversions. The electron and muon reconstruction efficiencies are $> 99\%$ for $p_T > 10 \text{ GeV}$.

The electron and muon candidates are required to satisfy isolation criteria in order to reject non-prompt leptons from the hadronisation process. Isolation is defined as the scalar sum of the p_T values of reconstructed charged and neutral particles within a cone of radius $\Delta R = \sqrt{(\Delta\eta)^2 + (\Delta\phi)^2} = 0.4$ around the lepton-candidate track, divided by the p_T of the lepton candidate. A correction is applied to the isolation variable to account for the effects of additional interactions. For charged particles, only tracks associated with the primary vertex are included in the isolation sums. The primary vertex is the reconstructed vertex with the largest sum of charged-track p_T^2 values associated to it. For neutral particles, a correction is applied by subtracting the energy deposited in the isolation cone by charged particles not associated with the primary vertex, multiplied by a factor of 0.5. This factor corresponds approximately to the ratio of neutral to charged hadron production in the hadronisation process of pileup interactions. In both cases, the contribution from the electron or muon candidate is removed from the sum and the value of the isolation variable is required to be 0.2 or less.

The muon identification-plus-isolation efficiency is 96% for muons with $p_T > 15 \text{ GeV}$ and $|\eta| <$

2.1. The rate at which pions undergoing $\pi^\pm \rightarrow \mu$ decay are misidentified as muons is 10^{-3} for pions with $p_T > 10$ GeV and $|\eta| < 2.1$. The electron identification-plus-isolation efficiency is 85% (80%) for electrons with $p_T > 30$ GeV in the barrel (endcap) region [31]. The $j \rightarrow e$ misidentification rate is 5×10^{-3} for jets with $p_T > 10$ GeV and $|\eta| < 2.1$.

Hadronic decays of τ leptons are reconstructed and identified using the hadrons-plus-strips algorithm [32], which is designed to optimize the performance of the τ_h reconstruction by considering specific τ_h decay modes. To suppress backgrounds in which light-quark or gluon jets can mimic τ_h decays, a τ_h candidate is required to be spatially isolated from other energy deposits in the event. The isolation variable is calculated using a multivariate boosted-decision-tree technique by forming rings of radius ΔR around the direction of the τ_h candidate, using the energy deposits of particles not considered in the reconstruction of the τ_h decay mode. Additionally, τ_h candidates are required to be distinguishable from electrons and muons in the event by using dedicated criteria based on the consistency among the measurements in the tracker, calorimeters, and muon detectors. The identification and isolation efficiency is 55–65% for a τ_h lepton with $p_T > 20$ GeV and $|\eta| < 2.1$, depending on the p_T and η values of the τ_h candidate. The rate at which jets are misidentified as a τ_h lepton is 1–5%, depending on the p_T and η values of the τ_h candidate.

The event selection criteria used in each search channel are summarized in Section 5 (see Table 1).

4 Signal and background samples

The composition of SM background events depends on the final state and, in particular, the number of τ_h candidates. The most important sources of background arise from the production of W or Z bosons in association with jets (W/Z+jets), and from $t\bar{t}$, diboson (VV: WW, WZ, ZZ), and Quantum ChromoDynamics (QCD) multijet events. The W+jets events are characterized by an isolated lepton from the decay of the W boson and uncorrelated jets misidentified as an e, μ , or τ_h . Background from W+jets events is especially pertinent for final states with one τ_h candidate. Background from $t\bar{t}$ events usually contains one or two tagged b quark jets, in addition to a genuine isolated e, μ , or τ_h .

Background from diboson events contains genuine, isolated leptons when the bosons decay leptonically, and jets that are misidentified as a τ_h lepton when they decay hadronically. The QCD background is characterized by jets that are misidentified as an e, μ , or τ_h lepton. The QCD multijet process is an appreciable background only for the $\tau_h\tau_h$ final states.

There are negligible contributions from background processes such as single-top and VBF production of a Higgs or Z boson. These background yields are taken from simulation.

Simulated samples of signal and background events are generated using Monte Carlo (MC) event generators. The signal event samples are generated with the MADGRAPH program (v5.1.5) [33], considering pair production of $\tilde{\chi}_1^\pm$ and $\tilde{\chi}_2^0$ gauginos ($\tilde{\chi}_1^\pm\tilde{\chi}_1^\pm$, $\tilde{\chi}_1^\pm\tilde{\chi}_1^\mp$, $\tilde{\chi}_1^\pm\tilde{\chi}_2^0$, and $\tilde{\chi}_2^0\tilde{\chi}_2^0$) with two associated partons. The signal events are generated requiring a pseudorapidity gap $|\Delta\eta| > 4.2$ between the two partons, with $p_T > 30$ GeV for each parton. Background event samples with a Higgs boson produced through VBF processes, and single top are generated with the POWHEG program (v1.0r1380) [34]. The MADGRAPH generator (v5.1.3) is used to describe Z+jets, W+jets, $t\bar{t}$, diboson, and VBF Z boson production.

The MC background and signal yields are normalized to the integrated luminosity of the data. The $t\bar{t}$ background is normalized to the next-to-next-to-leading-logarithm level using the cal-

culations of Refs. [35, 36]. The Z+jets and W+jets processes are normalized to next-to-next-to-leading-order using the results from the FEWZ v2.1 [37] generator. The diboson background processes are normalized to next-to-leading-order using the MCFM v5.8 [38] generator, while the VBF Z boson events are normalized to next-to-leading order using the VBFNLO (v2.6) [39] program. The single-top and VBF Higgs boson background yields are taken from the POWHEG program, where the next-to-leading order effects are incorporated. Signal cross sections are calculated at leading order using the MADGRAPH generator. All MC samples incorporate the CTEQ6L1 [40] or CTEQ6M [41] parton distribution functions (PDF). The corresponding evaluation of uncertainties in the signal cross sections is discussed in Section 7. The range of signal cross sections is 50–1 fb for $\tilde{\chi}_2^0 = \tilde{\chi}_1^\pm$ masses of 100–400 GeV. The POWHEG and MADGRAPH generators are interfaced with the PYTHIA (v6.4.22) [42] program, which is used to describe the parton shower and hadronisation processes. The decays of τ leptons are described using the TAUOLA (27.1215) [43] program.

The background samples are processed with a detailed simulation of the CMS apparatus using the GEANT4 package [44], while the response for signal samples is modeled with the CMS fast simulation program [45]. For the signal acceptance and m_{jj} shapes based on the fast simulation, the differences with respect to the GEANT4-based results are found to be small (<5%). Corrections are applied to account for the differences. For all MC samples, multiple proton-proton interactions are superimposed on the primary collision process, and events are reweighted such that the distribution of reconstructed collision vertices matches that in data. The distribution of the number of pileup interactions per event has a mean of 21 and a root-mean-square of 5.5.

5 Event selection

A single-muon trigger [30] with a p_T threshold of 24 GeV is used for the $\mu\mu jj$, $e\mu jj$, and $\mu\tau_h jj$ final states. The $\tau_h\tau_h jj$ channels use a double- τ_h trigger [46] that requires $p_T > 35$ GeV for each τ_h . A requirement on pseudorapidity ($|\eta| < 2.1$) is applied to select high quality and well-isolated leptons (e, μ , τ_h) within the tracker acceptance. The p_T thresholds defining the search regions are chosen to achieve a trigger efficiency greater than 90%. For final states with at least one muon ($\mu\mu jj$, $e\mu jj$, $\mu\tau_h jj$), events are selected by requiring a muon with $p_T > 30$ GeV. For the $\tau_h\tau_h$ channels, both τ_h candidates are required to satisfy $p_T > 45$ GeV.

The following requirements are referred to as the “central selection”, and are applied to all final states. Pairs of leptons are required to be separated by $\Delta R > 0.3$ and to originate from the primary vertex. All channels require exactly two leptons satisfying selection criteria. Events with an e or μ are required to have $p_T^{\text{miss}} > 75$ GeV, while a requirement $p_T^{\text{miss}} > 30$ GeV is used for the $\tau_h\tau_h jj$ final state to compensate for the loss in acceptance due to the higher p_T threshold of τ_h leptons while maintaining similar background rejection. Background from $t\bar{t}$ events is reduced by removing events in which any jet has $p_T > 20$ GeV, is separated from the leptons by $\Delta R > 0.3$, and is identified as b-quark jet using the loose working point of the CSV algorithm.

The “VBF selection” refers to the requirement of at least two jets in opposite hemispheres ($\eta_1\eta_2 < 0$) with large separation ($|\Delta\eta| > 4.2$). Events are selected with at least two jets with $p_T > 50$ GeV and pseudorapidity $|\eta| < 5.0$. The $\mu^\pm\mu^\pm jj$ search region has a lower background rate with respect to other final states, which makes it possible to relax the jet p_T requirement to 30 GeV to increase the signal acceptance. The event selection criteria with $p_T > 30$ GeV are referred to as “Loose”. The event selection criteria with $p_T > 50$ GeV are referred to as “Tight”. Selected events are required to have a dijet candidate with $m_{jj} > 250$ GeV.

The signal region (SR) is defined as the events that satisfy the central and VBF selection criteria.

A summary of the event selection criteria used in each channel is presented in Table 1.

Table 1: Summary of the event selection criteria for the different final states. The selections for the $\mu\mu jj$ and $e\mu jj$ channels are presented in one column ($\ell_{e/\mu}\mu jj$) as they are similar. The symbol ℓ_{e,μ,τ_h} means that the lepton could be an electron, a muon, or a τ_h lepton.

Selection	$\ell_{e/\mu}\mu jj$	$\mu\tau_h jj$	$\tau_h\tau_h jj$
$p_T(\mu)$ [GeV]	≥ 30	≥ 30	—
$p_T(\ell_{e/\mu})$ [GeV]	$\geq 15(e), \geq 10(\mu)$	—	—
$p_T(\tau_h)$ [GeV]	—	≥ 20	≥ 45
$ \eta(\ell_{\mu,e,\tau_h}) $	< 2.1	< 2.1	< 2.1
$N_{\text{jets}}^{\text{b-tag}}$	0	0	0
p_T^{miss} [GeV]	> 75	> 75	> 30
$p_T(\text{jets})$	$\geq 30/50$	≥ 50	≥ 30
$ \eta(\text{jets}) $	≤ 5	≤ 5	≤ 5
$ \Delta\eta(\text{jets}) $	> 4.2	> 4.2	> 4.2
$\eta_1\eta_2$	< 0	< 0	< 0

6 Background estimation

The general methodology used to evaluate the background is the same for all final states. We isolate various control regions (CR) to measure the VBF efficiencies (the probability for a given background component to satisfy the VBF selection criteria) and m_{jj} shapes from data, validate the modeling of the central selection criteria, and determine a correction factor to account for the selection efficiency by assessing the level of agreement between data and simulation. For each final state, the same trigger is used for the CRs as for the corresponding SR. The VBF efficiency, measured in a CR satisfying only the central selection, is defined as the fraction of events in the CR additionally passing the VBF event selection criteria.

The $t\bar{t}$, W +jets, and VV backgrounds are evaluated using the following equation:

$$N_{\text{BG}}^{\text{pred}}(m_{jj}) = N_{\text{BG}}^{\text{MC}}(\text{central}) SF_{\text{BG}}^{\text{CR1}}(\text{central}) \epsilon_{\text{VBF}}^{\text{CR2}}(m_{jj}), \quad (1)$$

where $N_{\text{BG}}^{\text{pred}}$ is the predicted background yield in the signal region, $N_{\text{BG}}^{\text{MC}}(\text{central})$ is the rate predicted by the “BG” simulation (with $\text{BG} = t\bar{t}, W$ +jets, or VV) for the central selection, $SF_{\text{BG}}^{\text{CR1}}(\text{central})$ is the data-to-simulation correction factor for the central region, given by the ratio of data to the “BG” simulation in control region CR1, and $\epsilon_{\text{VBF}}^{\text{CR2}}$ is the VBF efficiency, determined as a function of m_{jj} in data control sample CR2 or, in the case of VV events, from simulation.

The event selection criteria used to define the CR must not bias the m_{jj} distribution. This is verified, in simulation and data, by comparing the m_{jj} distributions with and without the selection criteria used to define the CR. The background estimation technique used to measure the VBF efficiency and m_{jj} shape from data is performed with simulated events to test the closure, where closure refers to the ability of the method to predict the correct background yields when using simulation in place of data. The closure tests demonstrate that the background determination techniques, described in detail below, reproduce the expected background distributions in both rate and shape to within the statistical uncertainties. The difference between the nominal MC background yields and the yields predicted from the closure test are added in quadrature with the statistical uncertainties of the prediction to define a systematic uncertainty. Simulated samples are further used to verify that the composition of objects erroneously

identified as leptons, and their kinematic properties, are similar between the CRs and SR, and thus that the scale factors S_{BG}^{CR1} (central) are unbiased. A variety of generators (MADGRAPH, PYTHIA, and POWHEG) are used for this purpose to establish the robustness of this expectation.

The production of $t\bar{t}$ events is an important source of background for the $\mu\mu jj$, $e\mu jj$, and $\mu\tau_h jj$ final states. Control regions enriched with $t\bar{t}$ events are obtained by requiring the presence of at least one reconstructed b-tagged jet with $p_T > 20$ GeV. The $t\bar{t}$ purity of the resulting data CR1s depends on the final state, ranging from 76 to 99%. The contributions of backgrounds other than $t\bar{t}$ events are subtracted from the data CR1s using simulation. The scale factors $S_{t\bar{t}}^{CR1}$ are then determined. The uncertainties related to the subtraction procedure are propagated to the scale factors. For the OS channels, the scale factors are consistent with unity to within 3%. The $t\bar{t}$ events with OS lepton pairs arise from genuine isolated leptons produced through leptonic W boson decay, and are well modeled by the simulation. On the other hand, $t\bar{t}$ events with SS lepton pairs mostly contain a lepton candidate that is a misidentified hadron or jet, which is more difficult to accurately simulate. The scale factors for SS events range from 1.2 to 1.5, with statistical uncertainties up to 25%. Since the fraction of lepton candidates that are in fact a misidentified hadron or jet varies according to the final state, the scale factors are determined independently for each channel. In contrast, the VBF efficiency for a given combination of lepton flavors does not depend on the charge state, and thus each pair of final states with the same flavor combination shares the same VBF efficiency value. The VBF efficiency is measured in data CR2 control samples obtained by additionally removing the charge requirement on the lepton pair and relaxing or inverting the lepton isolation requirement (isolation sidebands) in order to enhance the purity and statistical precision of the CR2s. Figure 2 shows the ‘‘Tight’’ and ‘‘Loose’’ VBF efficiencies measured from data, as a function of m_{jj} , for events in the $t\bar{t}$ CR2s of the $\mu\mu jj$ final states. The VBF efficiencies ϵ_{VBF}^{CR2} range from 0.02 to 0.003, with relative uncertainties below 11% for $m_{jj} > 250$ GeV. We verify that the b tagging, charge, and isolation requirements used to obtain the CR1 and CR2 samples do not bias the m_{jj} shape or the kinematic distributions of the leptons.

The production of W+jets events presents an important source of background only for the $\mu\tau_h jj$ search channels. Samples enriched in W+jets events, with about 70% purity according to simulation, are obtained by requiring the transverse mass $m_T \equiv \sqrt{2p_T^{\text{miss}} p_T^\mu [1 - \cos(\Delta\phi_{\mu, \vec{p}_T^{\text{miss}}})]}$ between \vec{p}_T^{miss} and the muon transverse momentum p_T^μ to satisfy $40 < m_T < 110$ GeV. The correction factor S_{W+jets}^{CR1} is determined to be 0.90 ± 0.11 , where the uncertainty is a combination of the statistical uncertainty from data, the statistical uncertainty from simulation, and the systematic uncertainty associated with the subtraction of the non-W+jets backgrounds from the data control sample. The lepton and τ_h isolation sidebands are used to obtain W+jets-enriched CR2 samples, with negligible expected signal contributions, not only to measure the VBF efficiencies and m_{jj} shape from data, but also to provide further validation of the S_{W+jets}^{CR1} correction factor. To validate the correction factor, the W+jets rate in the τ_h isolation sideband is scaled by 0.90 ± 0.11 , and agreement between the data and the corrected W+jets prediction from simulation is observed. The VBF efficiency determined from the CR2 control sample is measured to be $\approx 1\%$ for $m_{jj} > 250$ GeV. Agreement between the VBF efficiencies of Z+jets and W+jets processes is observed in the $\mu\tau_h jj$ channel.

The background from VV events is significant for final states containing only electrons and muons, comprising up to 10% of the total SM background in the OS channels, and up to 40% in the SS channels. The diboson background is suppressed in the τ_h final states because of the lower average p_T of the visible τ -lepton decay products. Diboson events have genuine isolated leptons and p_T^{miss} from neutrinos and can satisfy the VBF selection when produced in

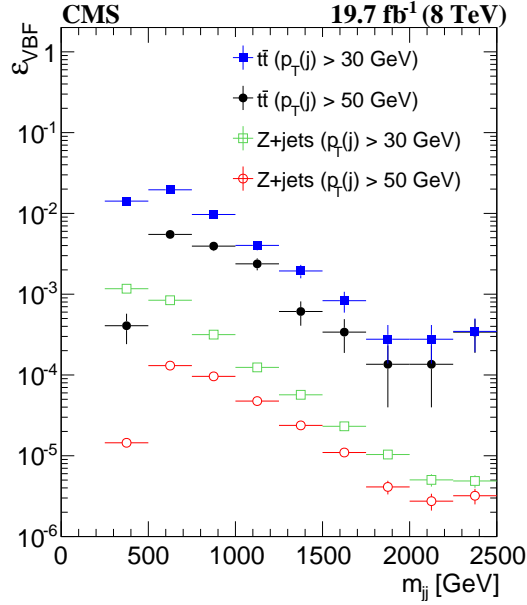


Figure 2: The VBF efficiency (see text) as a function of jet pair mass m_{jj} measured for the $t\bar{t}$ and Z+jets control regions of the $\mu\mu jj$ final state, for the “Loose” ($p_T > 30$ GeV) and “Tight” ($p_T > 50$ GeV) event selections.

association with jets arising from initial-state radiation or from a SM VBF process. We select diboson-enriched CR1 samples (97% purity) by requiring at least three leptons and inverting the p_T^{miss} requirement ($p_T^{\text{miss}} < 75$ GeV). The level of agreement between data and simulation for the event rates, VBF efficiencies, and m_{jj} shapes are found to be the same for all types of VV processes in the CR1 samples. The data-to-simulation correction factor is $SF_{VBF}^{\text{CR1}} = 1.12 \pm 0.06$. The m_{jj} distributions, following the VBF selections, are consistent between data and simulation. Therefore, the VBF efficiency is taken directly from simulation.

The Z+jets background is important for all OS final states. This background is evaluated using the following relation:

$$N_{Z+jets}^{\text{pred}}(m_{jj}) = N_{Z+jets}^{\text{MC}}(\text{central}) SF_{Z+jets}^{\text{CR1}}(\text{central}) SF_{p_T^{\text{miss}}}^{\text{CR3}} \epsilon_{VBF}^{\text{CR1}}(m_{jj}), \quad (2)$$

where N_{Z+jets}^{MC} , SF_{Z+jets}^{CR1} , and $\epsilon_{VBF}^{\text{CR1}}$ have the same meaning as the analogous quantities in Eq. (1) (with BG = Z+jets), and the $SF_{p_T^{\text{miss}}}^{\text{CR3}}$ term is described below. Control samples (CR1) dominated by $Z \rightarrow \ell\ell + \text{jets}$ events with $\ell = e, \mu$ (> 98% purity) are selected by requiring $p_T^{\text{miss}} < 75$ GeV and an OS lepton pair mass $m_{\ell\ell}$ consistent with the Z boson ($60 < m_{\ell\ell} < 120$ GeV). The rates and kinematic distributions of leptons in these control samples are consistent between the data and simulation. These control samples are used to determine both the SF_{Z+jets}^{CR1} correction factors and the $\epsilon_{VBF}^{\text{CR1}}$ terms, in the same manner as described above for the analogous quantities. The correction factors are unity to within 1%. Figure 2 shows the “Tight” and “Loose” VBF efficiencies measured from data, as a function of m_{jj} , for events in the $\mu\mu jj$ channel. The VBF efficiencies range from 10^{-3} to 10^{-5} . The measured $\epsilon_{VBF}^{\text{CR1}}$ terms agree with the results from simulation within 23%, which is taken as a systematic uncertainty both for the background prediction and for the VBF efficiency in simulated signal events. Additional orthogonal Z+jets control samples (CR3) are selected with similar selection criteria as used for the signal, maintaining the p_T^{miss} requirement (> 75 GeV) and inverting the VBF selection (i.e. at least one of the

VBF selection requirements is not satisfied: ≥ 2 jets, jet p_T , $|\Delta\eta|$, or $\eta_1\eta_2$). These control samples are used to determine the correction factors $SF_{p_T^{\text{miss}}}^{\text{CR3}}$, which account for differences between the data and simulation for high- p_T^{miss} events. The factors are 1.03 ± 0.03 (1.38 ± 0.10) for the τ_h (light-lepton flavor) channels. This mismodeling arises from the mismeasurement of p_T for jets and leptons.

High-purity samples of $Z \rightarrow \tau\tau \rightarrow \ell\tau_h$ events, from which the $SF_{Z+\text{jets}}^{\text{CR1}}$ terms can be evaluated for the search channels with at least one τ_h , are obtained by removing the VBF selection and requiring $m_T(\ell, p_T^{\text{miss}}) < 15$ GeV. The VBF efficiency for $Z \rightarrow \tau\tau+\text{jets}$ processes is obtained from data using the $Z \rightarrow \ell\ell+\text{jets}$ control samples described above.

The QCD multijet background is negligible for all final states except the $\tau_h\tau_h jj$ channel. To estimate the QCD multijet contribution to this channel, we select a QCD-dominated ($>90\%$ purity) CR1 by requiring two τ_h candidates with relaxed isolation requirements. In addition, we require that the CR1 events contain an SS $\tau_h\tau_h$ pair. The SS signal region is thus included in CR1, but the potential impact of signal events is found to be negligible. The QCD multijet background in the OS $\tau_h\tau_h$ channel is estimated by:

$$N_{\text{QCD}}^{\text{pred}}(m_{jj}) = N_{\text{QCD}}^{\text{CR1}}(\text{central}) R_{\text{OS/SS}} \epsilon_{\text{VBF}}^{\text{CR2}}(m_{jj}), \quad (3)$$

where $N_{\text{QCD}}^{\text{CR1}}(\text{central})$ is the yield observed in the CR1 sample with no VBF requirements, following subtraction of the non-QCD component from CR1 using simulation. The OS-to-SS ratio $R_{\text{OS/SS}}$ is obtained from a low- p_T^{miss} ($p_T^{\text{miss}} < 30$ GeV) region after subtraction of the non-QCD contributions: we find $R_{\text{OS/SS}} = 1.33 \pm 0.03$. Besides its use in the background determination procedure [Eq. (3)], the measured result for $R_{\text{OS/SS}}$ is used to provide a cross-check: we use it to extrapolate from an SS to an OS control region, both selected requiring $p_T^{\text{miss}} < 30$ GeV and two non-isolated τ_h candidates. The obtained prediction for the rate of non-isolated OS τ_h leptons is in agreement with the observation. Finally, the efficiency $\epsilon_{\text{VBF}}^{\text{CR2}}$ is measured in exclusive sidebands fulfilling inverted τ_h isolation criteria. It is estimated as the rate of events with two non-isolated τ_h candidates plus two jets satisfying the VBF requirements divided by the rate of events with two non-isolated τ_h candidates without any additional jet requirements. The measured efficiency is $\epsilon_{\text{VBF}} = 0.35\% \pm 0.08\%$ (stat) $\pm 0.06\%$ (syst).

The QCD multijet background in the SS $\tau_h\tau_h jj$ channel is estimated using the following relation:

$$N_{\text{QCD}}^{\text{pred}} = N_{\text{QCD}}^{\text{fail-VBF}} \frac{\epsilon_{\text{VBF}}^{\text{non-iso}\tau_h}}{1 - \epsilon_{\text{VBF}}^{\text{non-iso}\tau_h}}. \quad (4)$$

Here, $N_{\text{QCD}}^{\text{fail-VBF}}$ is the observed yield in data, with non-QCD background from simulation subtracted, in an SS $\tau_h\tau_h$ control sample requiring at least two jets not associated with one of the τ_h candidates to fail any of the $|\Delta\eta|$, $\eta_1\eta_2$, or m_{jj} requirements. The VBF efficiency $\epsilon_{\text{VBF}}^{\text{non-iso}\tau_h}$ (ϵ_{VBF} for short) is measured in six exclusive τ_h isolation sidebands, without a p_T^{miss} requirement and at least two jets. The validity of the method is demonstrated in data by the agreement that is observed, within statistical uncertainties, of these six independent measurements of ϵ_{VBF} . The six corresponding control samples in simulation are used to test the stability of ϵ_{VBF} as a function of p_T^{miss} and the τ_h isolation requirements. For this purpose, the probability for a single jet to be misidentified as a τ_h lepton is determined from simulation. The misidentification rates depend on the jet p_T and are used to determine an overall event weight by randomly selecting two jets in the event to represent the τ_h leptons. The VBF efficiencies in simulation are calculated from these weighted samples and demonstrate consistency with respect to the

different p_T^{miss} and τ_h isolation requirements at the level of $\approx 19\%$, which is assigned as a systematic uncertainty in the background prediction. The VBF efficiency for $m_{jj} > 250$ GeV is $\epsilon_{\text{VBF}} = 6.7\% \pm 0.5\%$ (stat) $_{-0.5\%}^{+1.2\%}$ (syst).

7 Systematic uncertainties

The main contributions to the total systematic uncertainty in the background predictions arise from the closure tests and from the statistical uncertainties associated with the data control regions used to determine the $\epsilon_{\text{VBF}}^{\text{CR}}$, $SF_{\text{BG}}^{\text{CR1}}$ (central), and $R_{\text{OS/SS}}$ factors. The relative systematic uncertainties in $SF_{\text{BG}}^{\text{CR1}}$ and $R_{\text{OS/SS}}$ related to the statistical precision in the CRs range between 1 and 25%, depending on the background component and search channel. For $m_{jj} > 250$ GeV, the statistical uncertainties in $\epsilon_{\text{VBF}}^{\text{CR}}$ lie between 3 and 21%, while the systematic uncertainties evaluated from the closure tests and cross-checks with data range from 2 to 20%. For the background $\epsilon_{\text{VBF}}^{\text{CR}}$, we assign no uncertainty due to the jet energy correction, as the m_{jj} distributions are taken directly from the data control regions.

Less significant contributions to the systematic uncertainties arise from contamination by non-targeted background sources to the CRs used to measure $\epsilon_{\text{VBF}}^{\text{CR}}$, and from the uncertainties in $SF_{\text{BG}}^{\text{CR1}}$ (central) due to the lepton identification efficiency, lepton energy and momentum scales, p_T^{miss} scale, and trigger efficiency.

The efficiencies for the electron and muon trigger, reconstruction, identification, and isolation requirements are measured with the “tag-and-probe” method [30, 31] with a resulting uncertainty of 2%. The τ_h trigger and identification-plus-isolation efficiencies are measured from a fit to the $Z \rightarrow \tau\tau \rightarrow \mu\tau_h$ visible mass distribution in a sample selected with a single-muon trigger, leading to a relative uncertainty of 4% and 6% per τ_h candidate, respectively [46]. The p_T^{miss} scale uncertainties contribute via the jet energy scale (2–10% depending on η and p_T) and unclustered energy scale (10%) uncertainties, where “unclustered energy” refers to energy from a reconstructed object that is not assigned to a jet with $p_T > 10$ GeV or to a lepton with $p_T > 10$ GeV.

Since the estimate of the background is partly based on simulation, the signal and background rates are affected by similar sources of systematic uncertainty, such as the luminosity uncertainty of 2.6% [47]. The uncertainties in the lepton identification efficiency, lepton energy and momentum scale, p_T^{miss} scale, and trigger efficiency also contribute to the systematic uncertainty in the signal.

The signal event acceptance for the VBF selection depends on the reconstruction and identification efficiency and jet energy scale of forward jets. The jet reconstruction-plus-identification efficiency is $>98\%$ for the entire η and p_T range, as is validated through the agreement observed between data and simulation in the η distribution of jets, in particular at high η , in control samples enriched with $t\bar{t}$ background events. The dominant uncertainty in the signal acceptance is due to the modelling of the kinematic properties of jets, and thus the VBF efficiency, for forward jets in the MADGRAPH simulation. This is investigated by comparing the predicted and measured m_{jj} spectra in the Z+jets CRs. The level of agreement between the predicted and observed m_{jj} spectra is better than 23%, which is assigned as a systematic uncertainty in the VBF efficiency for signal samples. The uncertainty in the signal acceptance due to the PDF set included in the simulated samples is evaluated in accordance with the PDF4LHC recommendations [48, 49] by comparing the results obtained using the CTEQ6.6L, MSTW08, and NNPDF10 PDF sets [41, 50, 51] with those from the default PDF set (CTEQ6L1). The dominant uncertainties that contribute to the m_{jj} shape variations include the p_T^{miss} and jet energy

scale uncertainties. Correlations of the uncertainty sources are discussed in Section 8.

8 Results and interpretation

Figures 3 and 4 present the data in comparison to the predicted SM background. The combined results from all channels are shown in Fig. 5. Numerical results are given in Tables 2 and 3. The observed numbers of events are seen to be consistent with the expected SM background in all search regions. Therefore the search does not reveal any evidence for new physics.

Table 2: Number of observed events and corresponding background predictions for the OS channels. The uncertainties are statistical, including the statistical uncertainties from the control regions and simulated event samples.

Process	$\mu^\pm\mu^\mp jj$	$e^\pm\mu^\mp jj$	$\mu^\pm\tau_h^\mp jj$	$\tau_h^\pm\tau_h^\mp jj$
Z+jets	4.3 ± 1.7	$3.7^{+2.1}_{-1.9}$	19.9 ± 2.9	12.3 ± 4.4
W+jets	<0.1	$4.2^{+3.3}_{-2.5}$	17.3 ± 3.0	2.0 ± 1.7
VV	2.8 ± 0.5	3.1 ± 0.7	2.9 ± 0.5	0.5 ± 0.2
$t\bar{t}$	24.0 ± 1.7	$19.0^{+2.3}_{-2.4}$	11.7 ± 2.8	—
QCD	—	—	—	6.3 ± 1.8
Higgs boson	1.0 ± 0.1	1.1 ± 0.5	—	1.1 ± 0.1
VBF Z	—	—	—	0.7 ± 0.2
Total	32.2 ± 2.4	$31.1^{+4.6}_{-4.1}$	51.8 ± 5.1	22.9 ± 5.1
Observed	31	22	41	31

Table 3: Number of observed events and corresponding background predictions for the SS channels. The uncertainties are statistical, including the statistical uncertainties from the control regions and simulated event samples.

Process	$\mu^\pm\mu^\pm jj$	$e^\pm\mu^\pm jj$	$\mu^\pm\tau_h^\pm jj$	$\tau_h^\pm\tau_h^\pm jj$
Z+jets	<0.1	$0^{+1.7}_{-0}$	0.5 ± 0.2	<0.1
W+jets	<0.1	$0^{+3.0}_{-0}$	9.3 ± 2.3	0.5 ± 0.1
VV	2.1 ± 0.3	$1.9^{+0.4}_{-0.2}$	1.1 ± 0.2	$0.1 \pm 6.5 \times 10^{-2}$
$t\bar{t}$	3.1 ± 0.1	$3.5^{+0.7}_{-0.9}$	6.7 ± 2.8	$0.1 \pm 1.2 \times 10^{-2}$
Single top	—	—	—	<0.1
QCD	—	—	—	7.6 ± 0.9
Higgs boson	—	—	—	<0.1
Total	5.4 ± 0.3	$5.4^{+3.5}_{-0.9}$	17.6 ± 3.8	8.4 ± 0.9
Observed	4	5	14	9

To quantify the sensitivity of this search, the results are interpreted in the context of the R-parity conserving minimal supersymmetric SM by considering production of charginos and neutralinos with two associated jets, as described in Section 4. Models with a bino-like $\tilde{\chi}_1^0$ and wino-like $\tilde{\chi}_2^0$ and $\tilde{\chi}_1^\pm$ are considered. Since the $\tilde{\chi}_2^0$ and $\tilde{\chi}_1^\pm$ belong to the same gauge group multiplet, we set $m_{\tilde{\chi}_2^0} = m_{\tilde{\chi}_1^\pm}$ and present results as a function of this common mass and the LSP mass $m_{\tilde{\chi}_1^0}$. In the presence of a light slepton, $\tilde{\ell} = \tilde{e}/\tilde{\mu}/\tilde{\tau}$, it is likely that the $\tilde{\chi}_1^\pm$ will decay to $\ell\nu\tilde{\chi}_1^0$ and the $\tilde{\chi}_2^0$ to $\ell^+\ell^-\tilde{\chi}_1^0$. The results are interpreted by considering $\tilde{\ell} = \tilde{\tau}$ and assuming branching fractions $\mathcal{B}(\tilde{\chi}_2^0 \rightarrow \tau\tilde{\tau} \rightarrow \tau\tau\tilde{\chi}_1^0) = 1$ and $\mathcal{B}(\tilde{\chi}_1^\pm \rightarrow \nu\tilde{\tau} \rightarrow \nu\tau\tilde{\chi}_1^0) = 1$. To highlight how the VBF searches described in this paper complement other searches for the electroweak production of SUSY particles [17, 18], two scenarios are considered: (i) $m_{\tilde{\chi}_1^0} = 0$ GeV (uncompressed-mass spectrum) and (ii) $m_{\tilde{\chi}_1^\pm} - m_{\tilde{\chi}_1^0} = 50$ GeV (compressed-mass spectrum).

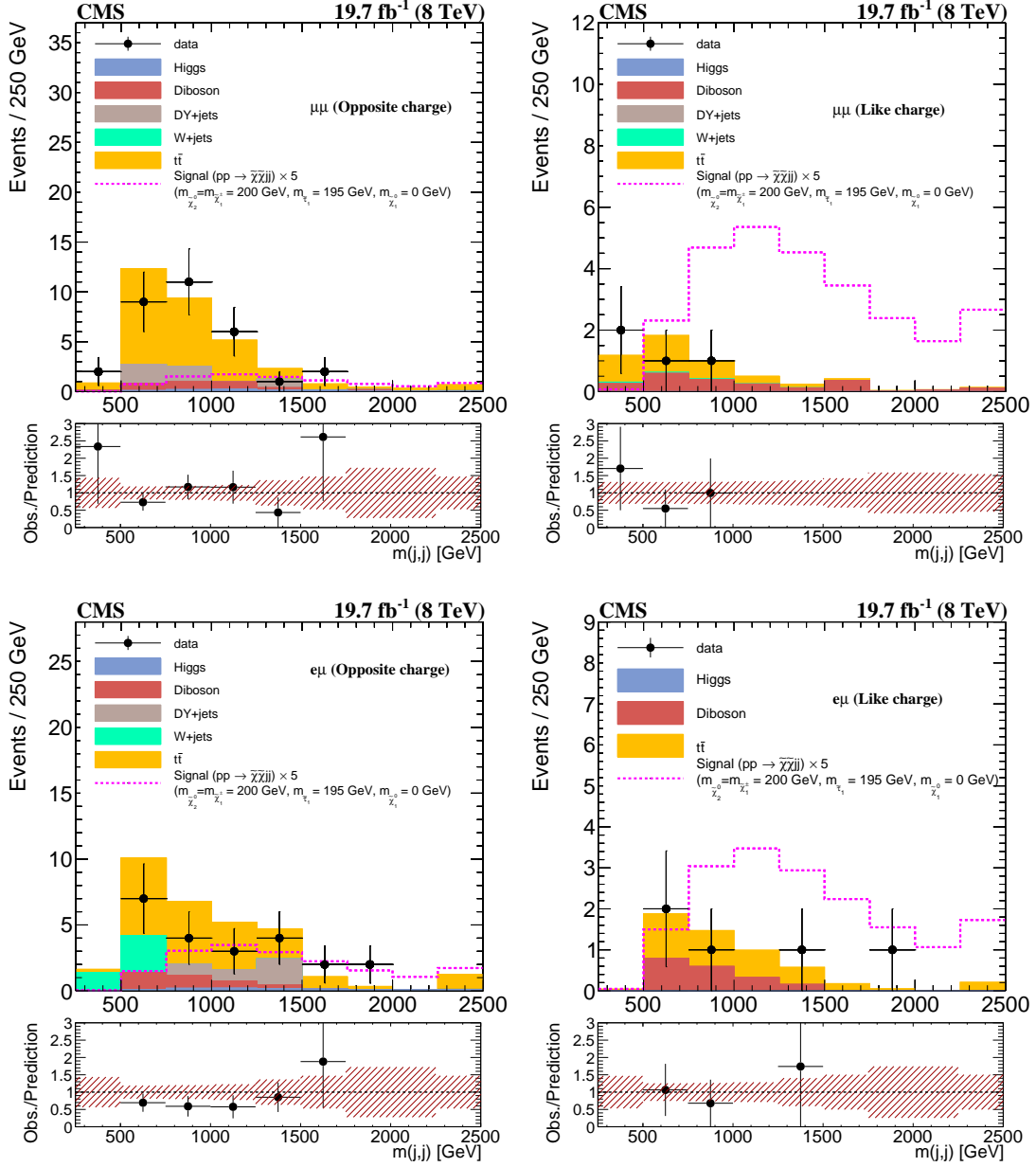


Figure 3: Dijet invariant mass distributions in the (upper left) OS $\mu\mu$, (upper right) SS $\mu\mu$, (lower left) OS $e\mu$, and (lower right) SS $e\mu$ signal regions. The signal scenario with $m_{\tilde{\chi}_2^0} = m_{\tilde{\chi}_1^\pm} = 200$ GeV, $m_{\tilde{\tau}} = 195$ GeV, and $m_{\tilde{\chi}_1^0} = 0$ GeV, as described in Section 4, is shown. The signal events are scaled up by a factor of 5 for purposes of visibility. The shaded band in the ratio plot includes the systematic and statistical uncertainties in the background prediction.

The cumulative signal event acceptance is shown in Table 4 at three stages of the analysis: accounting for the branching fractions for the SUSY event to yield the indicated two-lepton channel (BF), the acceptance following application of the central selection (Central), and the acceptance following the VBF selection (VBF). The average p_T values of the e , μ , and τ_h objects in signal events are relatively soft, because of the energy and momentum carried by the associated neutrinos in the τ decays. The OS and SS channels have similar signal acceptance because lepton pairs satisfying the event selection do not necessarily originate from the $\tilde{\chi}_2^0$ or $\tilde{\chi}_1^\pm \tilde{\chi}_1^\mp$ decays. The best signal sensitivity comes from the SS $\mu\mu$ and $e\mu$ channels due to a better

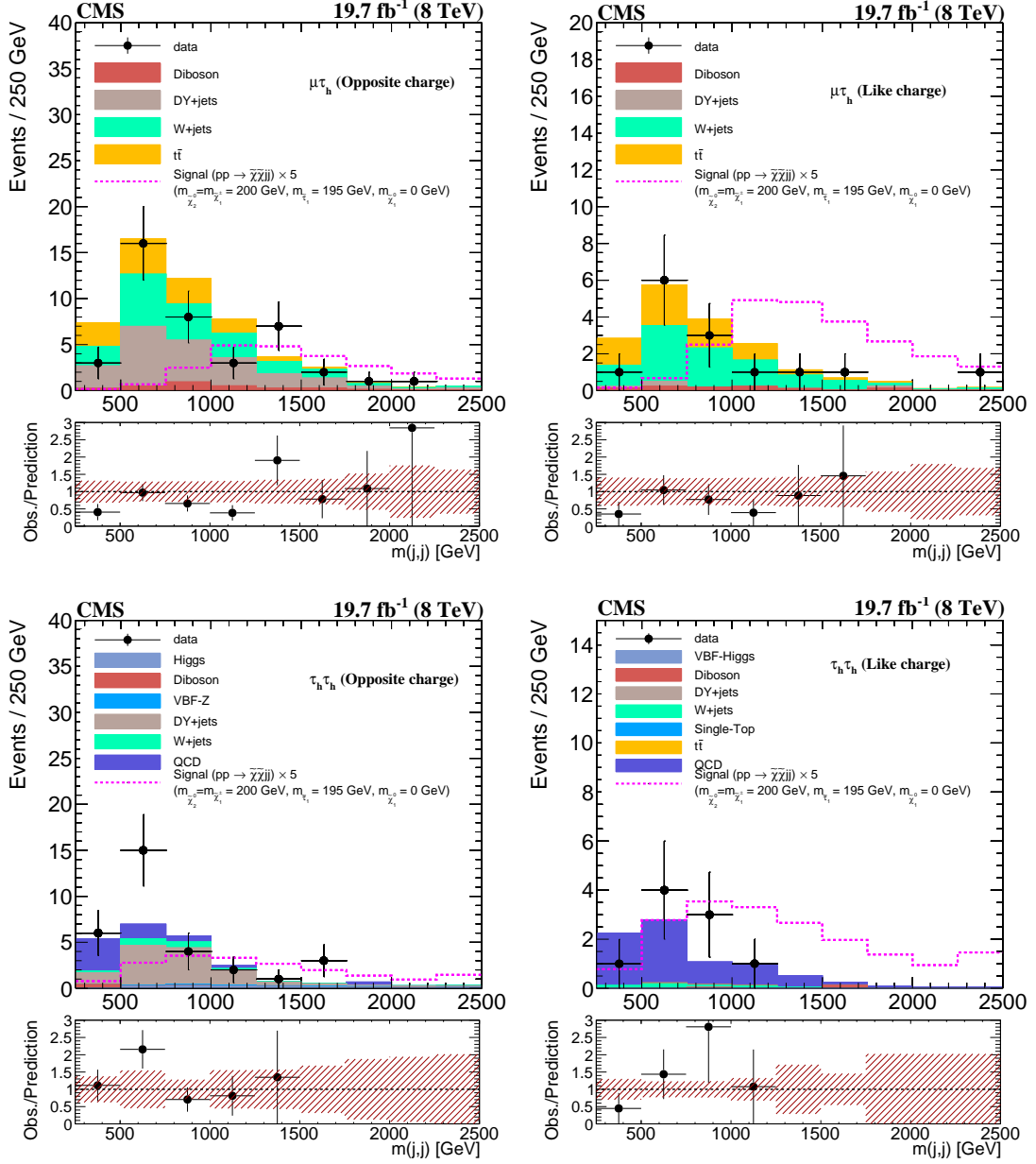


Figure 4: Dijet invariant mass distributions in the (upper left) OS $\mu\tau_h$, (upper right) SS $\mu\tau_h$, (lower left) OS $\tau_h\tau_h$, and (lower right) SS $\tau_h\tau_h$ signal regions. The signal scenario with $m_{\tilde{\chi}_2^0} = m_{\tilde{\chi}_1^\pm} = 200$ GeV, $m_{\tilde{\tau}} = 195$ GeV, and $m_{\tilde{\chi}_1^0} = 0$ GeV, as described in Section 4, is shown. The signal events are scaled up by a factor of 5 for purposes of visibility. The shaded band in the ratio plot includes the systematic and statistical uncertainties in the background prediction.

background suppression with respect to a given signal acceptance.

The expected signal yields from simulation with $m_{\tilde{\chi}_1^0} = 0$ GeV and $\Delta m(\tilde{\chi}_1^\pm, \tilde{\chi}_1^0) = 50$ GeV, are presented in Table 5. The signal acceptance depends on the mass $m_{\tilde{\tau}}$ of the intermediate τ slepton. The results in Table 5 are presented under two different assumptions for $m_{\tilde{\tau}}$: (i) a fixed-mass difference assumption $\Delta m(\tilde{\chi}_1^\pm, \tilde{\tau}) = 5$ GeV, and (ii) an average-mass assumption $m_{\tilde{\tau}} = 0.5m_{\tilde{\chi}_1^\pm} + 0.5m_{\tilde{\chi}_1^0}$. In the compressed-mass-spectrum scenario, for which $m_{\tilde{\chi}_1^\pm} - m_{\tilde{\chi}_1^0} = 50$ GeV, the average-mass assumption yields significantly lower average lepton p_T than the

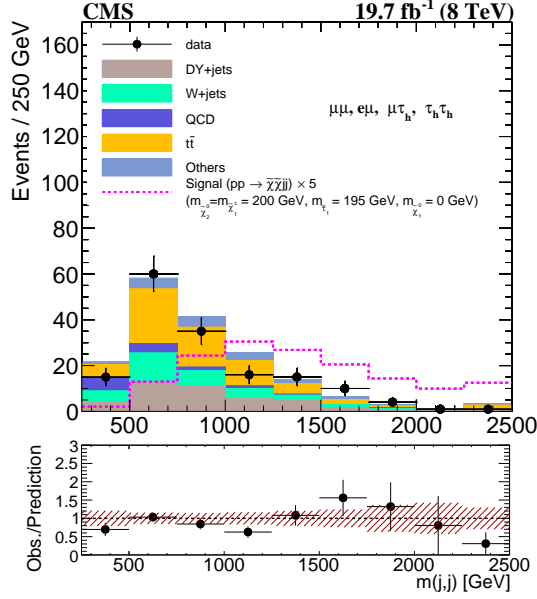


Figure 5: Dijet invariant mass distribution for the combination of all search channels. The signal scenario with $m_{\tilde{\chi}_2^0} = m_{\tilde{\chi}_1^\pm} = 200$ GeV, $m_{\tilde{\tau}} = 195$ GeV, and $m_{\tilde{\chi}_1^0} = 0$ GeV, as described in Section 4, is shown. The signal events are scaled up by a factor of 5 for purposes of visibility. The shaded band in the ratio plot includes the systematic and statistical uncertainties in the background prediction.

fixed-mass assumption, and the acceptance is lower by a factor of 2–3. In the uncompressed-mass-spectrum scenario, with $m_{\tilde{\chi}_1^0} = 0$ GeV, the average-mass assumption produces larger average lepton p_T than the fixed-mass assumption, yielding an event acceptance that is 1.3–1.8 times larger.

Table 4: Cumulative signal event acceptance after application of the BF, central, and VBF requirements (see text). Note that the jet p_T threshold for the $\mu\mu jj$ and $\tau_h\tau_h jj$ final states is 30 GeV, while it is 50 GeV for the other final states.

Channel	BF($\geq 1l_1$ & $\geq 1l_2$)	Central	VBF
$\mu^\pm\tau_{th}^\mp$ ($\mu^\pm\tau_{th}^\pm$)	0.399	0.020 (0.020)	0.007 (0.007)
$e^\pm\mu^\mp$ ($e^\pm\mu^\pm$)	0.152	0.037 (0.037)	0.014 (0.014)
$\tau_{th}^\pm\tau_{th}^\mp$ ($\tau_{th}^\pm\tau_{th}^\pm$)	0.717	0.010 (0.010)	0.009 (0.009)
$\mu^\pm\mu^\mp$ ($\mu^\pm\mu^\pm$)	0.081	0.018 (0.018)	0.007 (0.017)

The calculation of the exclusion limit is obtained by using the m_{jj} distribution in each channel to construct a combined likelihood in bins of m_{jj} and computing a 95% confidence level (CL) upper limit on the signal cross section using the asymptotic CL_s criterion [52–54]. Systematic uncertainties are taken into account as nuisance parameters, which are removed by marginalization, assuming a gamma or log-normal prior for normalization parameters, and Gaussian priors for mass spectrum shape uncertainties. The combination of the eight search channels requires simultaneous analysis of the data from the individual channels, accounting for all statistical and systematic uncertainties and their correlations. Correlations among backgrounds, both within a channel and across channels, are taken into consideration in the limit calculation. For example, the uncertainties in physics object identification and reconstruction are treated as correlated for channels with a common particle in their final states, while the uncertainty in the integrated luminosity is treated as correlated across channels. The uncertainties resulting

Table 5: Signal event yields from simulation. The first terms $\{m_{\tilde{\chi}_1^\pm}, m_{\tilde{\tau}}\}$ correspond to the fixed-mass difference assumption $\Delta m(\tilde{\chi}_1^\pm, \tilde{\tau}) = 5 \text{ GeV}$, while the terms in parentheses ($\{m_{\tilde{\chi}_1^\pm}, m_{\tilde{\tau}}\}$) correspond to the average-mass assumption $m_{\tilde{\tau}} = 0.5m_{\tilde{\chi}_1^0} + 0.5m_{\tilde{\chi}_1^\pm}$.

$\{m(\tilde{\chi}_1^\pm), m(\tilde{\tau})\} [\text{GeV}]$	$\mu^\pm \mu^\pm jj$ (loose)	$\mu^\pm \mu^\mp jj$ (tight)	$e\mu jj$	$\mu \tau_h jj$	$\tau_h \tau_h jj$
$m(\tilde{\chi}_1^0) = 0 \text{ GeV}$					
$\{100, 95\} (\{100, 50\})$	16(29)	6.6(12)	13(24)	7.1(9.4)	8.7(10.7)
$\{200, 195\} (\{200, 100\})$	5.4(9.7)	1.8(3.1)	3.5(6.3)	4.5(6.0)	3.8(4.7)
$\{300, 295\} (\{300, 150\})$	2.3(4.1)	0.68(1.2)	1.4(2.4)	1.9(2.5)	1.5(2.0)
$\{400, 395\} (\{400, 200\})$	0.57(1.0)	0.17(0.30)	0.35(0.62)	0.46(0.63)	0.38(0.51)
$\Delta m(\tilde{\chi}_1^\pm - \tilde{\chi}_1^0) = 50 \text{ GeV}$					
$\{200, 195\} (\{200, 175\})$	1.4(0.5)	0.85(0.33)	1.7(0.65)	0.99(0.35)	0.46(0.09)
$\{300, 295\} (\{300, 275\})$	0.47(0.18)	0.28(0.11)	0.58(0.23)	0.40(0.14)	0.20(0.04)
$\{400, 395\} (\{400, 375\})$	0.12(0.05)	0.08(0.03)	0.15(0.06)	0.10(0.03)	0.05(0.01)

from the number of simulated events, and from the event acceptance variation with different sets of PDFs in a given m_{jj} bin, are treated as uncorrelated within a channel and correlated across channels. The uncertainties due to the closure tests are treated as uncorrelated within and across the different final states.

Figures 6 (left) and 6 (right) show the expected and observed limits as well as the theoretical cross section as functions of $m_{\tilde{\chi}_1^\pm}$ for, respectively, the fixed- and average-mass $m_{\tilde{\tau}}$ assumptions. For the fixed-mass assumption with a compressed-mass spectrum ($m_{\tilde{\chi}_1^\pm} - m_{\tilde{\chi}_1^0} = 50 \text{ GeV}$), $\tilde{\chi}_2^0$ and $\tilde{\chi}_1^\pm$ gauginos with masses below 170 GeV are excluded, where the previous ATLAS and CMS SUSY searches do not probe. For the average-mass assumption with an uncompressed-mass spectrum ($m_{\tilde{\chi}_1^0} = 0$), the corresponding limit is 300 GeV. These mass limits are conservatively determined using the theoretical cross section minus its one standard deviation uncertainty. The $m_{\tilde{\chi}_1^\pm}$ limits of 320 and 380 GeV for $m_{\tilde{\chi}_1^0} = 0 \text{ GeV}$ in Refs. [17, 18] can be compared to the corresponding result of 300 GeV in the present analysis [see the yellow band in Fig. 6 (right)].

9 Summary

A search is presented for non-coloured supersymmetric particles in the vector-boson fusion (VBF) topology using data corresponding to an integrated luminosity of 19.7 fb^{-1} collected with the CMS detector in proton-proton collisions at $\sqrt{s} = 8 \text{ TeV}$. This is the first search for SUSY in the VBF topology. The search utilizes events in eight different final states covering both same- and opposite-sign dilepton pairs. The leptons considered are electrons, muons, and hadronically decaying τ leptons. The VBF topology requires two well-separated jets that appear in opposite hemispheres, with large invariant mass m_{jj} . The observed m_{jj} distributions do not reveal any evidence for new physics. The results are used to exclude a range of $\tilde{\chi}_1^\pm$ and $\tilde{\chi}_2^0$ gaugino masses. For models in which the $\tilde{\chi}_1^0$ lightest-supersymmetric-particle mass is zero, and in which the $\tilde{\chi}_1^\pm$ and $\tilde{\chi}_2^0$ branching fractions to τ leptons are large, $\tilde{\chi}_1^\pm$ and $\tilde{\chi}_2^0$ masses up to 300 GeV are excluded at 95% CL. For a compressed-mass-spectrum scenario, in which $m_{\tilde{\chi}_1^\pm} - m_{\tilde{\chi}_1^0} = 50 \text{ GeV}$, the corresponding limit is 170 GeV. While many previous studies at the LHC have focused on strongly coupled supersymmetric particles, including searches for charginos and neutralinos produced in gluino or squark decay chains, and a number of studies have presented limits on the Drell-Yan production of charginos and neutralinos, this analysis obtains

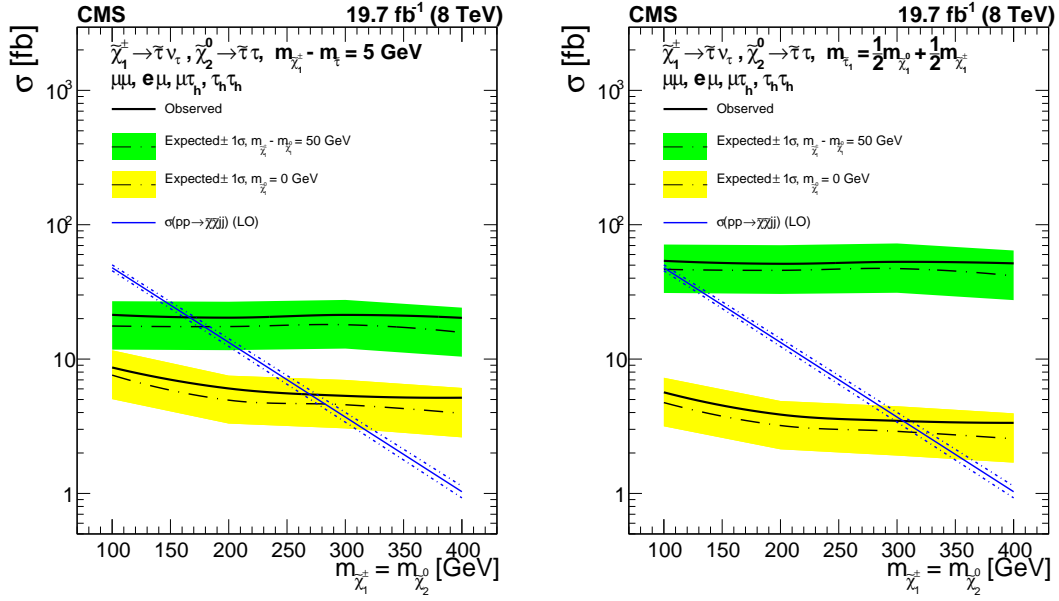


Figure 6: Combined 95% CL upper limits on the cross section as a function of $m_{\tilde{\chi}_2^0} = m_{\tilde{\chi}_1^\pm}$. The signal cross section is calculated with the VBF jet selection: jet $p_T > 30$ GeV, $|\Delta\eta(\text{jets})| > 4.2$, and $\eta_1\eta_2 < 0$. (left) The results for the fixed-mass difference assumption, in which $m_{\tilde{\chi}_1^\pm} - m_{\tilde{\chi}_1^0} = 5$ GeV, for $m_{\tilde{\chi}_1^\pm} - m_{\tilde{\chi}_1^0} = 50$ GeV (compressed-mass spectrum) and $m_{\tilde{\chi}_1^0} = 0$ GeV (uncompressed-mass spectrum). (right) The corresponding results for the average-mass assumption, in which $m_{\tilde{\tau}} = 0.5m_{\tilde{\chi}_1^\pm} + 0.5m_{\tilde{\chi}_1^0}$.

the most stringent limits to date on the production of charginos and neutralinos decaying to τ leptons in compressed-mass-spectrum scenarios defined by the mass separation $\Delta m = m_{\tilde{\chi}_1^\pm} - m_{\tilde{\chi}_1^0} < 50$ GeV.

Acknowledgments

We congratulate our colleagues in the CERN accelerator departments for the excellent performance of the LHC and thank the technical and administrative staffs at CERN and at other CMS institutes for their contributions to the success of the CMS effort. In addition, we gratefully acknowledge the computing centres and personnel of the Worldwide LHC Computing Grid for delivering so effectively the computing infrastructure essential to our analyses. Finally, we acknowledge the enduring support for the construction and operation of the LHC and the CMS detector provided by the following funding agencies: the Austrian Federal Ministry of Science, Research and Economy and the Austrian Science Fund; the Belgian Fonds de la Recherche Scientifique, and Fonds voor Wetenschappelijk Onderzoek; the Brazilian Funding Agencies (CNPq, CAPES, FAPERJ, and FAPESP); the Bulgarian Ministry of Education and Science; CERN; the Chinese Academy of Sciences, Ministry of Science and Technology, and National Natural Science Foundation of China; the Colombian Funding Agency (COLCIENCIAS); the Croatian Ministry of Science, Education and Sport, and the Croatian Science Foundation; the Research Promotion Foundation, Cyprus; the Ministry of Education and Research, Estonian Research Council via IUT23-4 and IUT23-6 and European Regional Development Fund, Estonia; the Academy of Finland, Finnish Ministry of Education and Culture, and Helsinki Institute of Physics; the Institut National de Physique Nucléaire et de Physique des Particules / CNRS, and Commissariat à l'Énergie Atomique et aux Énergies Alternatives / CEA,

France; the Bundesministerium für Bildung und Forschung, Deutsche Forschungsgemeinschaft, and Helmholtz-Gemeinschaft Deutscher Forschungszentren, Germany; the General Secretariat for Research and Technology, Greece; the National Scientific Research Foundation, and National Innovation Office, Hungary; the Department of Atomic Energy and the Department of Science and Technology, India; the Institute for Studies in Theoretical Physics and Mathematics, Iran; the Science Foundation, Ireland; the Istituto Nazionale di Fisica Nucleare, Italy; the Ministry of Science, ICT and Future Planning, and National Research Foundation (NRF), Republic of Korea; the Lithuanian Academy of Sciences; the Ministry of Education, and University of Malaya (Malaysia); the Mexican Funding Agencies (CINVESTAV, CONACYT, SEP, and UASLP-FAI); the Ministry of Business, Innovation and Employment, New Zealand; the Pakistan Atomic Energy Commission; the Ministry of Science and Higher Education and the National Science Centre, Poland; the Fundação para a Ciência e a Tecnologia, Portugal; JINR, Dubna; the Ministry of Education and Science of the Russian Federation, the Federal Agency of Atomic Energy of the Russian Federation, Russian Academy of Sciences, and the Russian Foundation for Basic Research; the Ministry of Education, Science and Technological Development of Serbia; the Secretaría de Estado de Investigación, Desarrollo e Innovación and Programa Consolider-Ingenio 2010, Spain; the Swiss Funding Agencies (ETH Board, ETH Zurich, PSI, SNF, UniZH, Canton Zurich, and SER); the Ministry of Science and Technology, Taipei; the Thailand Center of Excellence in Physics, the Institute for the Promotion of Teaching Science and Technology of Thailand, Special Task Force for Activating Research and the National Science and Technology Development Agency of Thailand; the Scientific and Technical Research Council of Turkey, and Turkish Atomic Energy Authority; the National Academy of Sciences of Ukraine, and State Fund for Fundamental Researches, Ukraine; the Science and Technology Facilities Council, UK; the US Department of Energy, and the US National Science Foundation.

Individuals have received support from the Marie-Curie programme and the European Research Council and EPLANET (European Union); the Leventis Foundation; the A. P. Sloan Foundation; the Alexander von Humboldt Foundation; the Belgian Federal Science Policy Office; the Fonds pour la Formation à la Recherche dans l'Industrie et dans l'Agriculture (FRIA-Belgium); the Agentschap voor Innovatie door Wetenschap en Technologie (IWT-Belgium); the Ministry of Education, Youth and Sports (MEYS) of the Czech Republic; the Council of Science and Industrial Research, India; the HOMING PLUS programme of the Foundation for Polish Science, cofinanced from European Union, Regional Development Fund; the OPUS programme of the National Science Center (Poland); the Compagnia di San Paolo (Torino); the Consorzio per la Fisica (Trieste); MIUR project 20108T4XTM (Italy); the Thalís and Aristeia programmes cofinanced by EU-ESF and the Greek NSRF; the National Priorities Research Program by Qatar National Research Fund; the Rachadapisek Sompot Fund for Postdoctoral Fellowship, Chulalongkorn University (Thailand); and the Welch Foundation, contract C-1845.

References

- [1] P. Ramond, "Dual Theory for Free Fermions", *Phys. Rev. D* **3** (1971) 2415, doi:10.1103/PhysRevD.3.2415.
- [2] Y. A. Gol'fand and E. P. Likhtman, "Extension of the algebra of Poincaré group generators and violation of P invariance", *JETP Lett.* **13** (1971) 323.
- [3] S. Ferrara and B. Zumino, "Supergauge invariant Yang-Mills theories", *Nucl. Phys. B* **79** (1974) 413, doi:10.1016/0550-3213(74)90559-8.

- [4] J. Wess and B. Zumino, "Supergauge transformations in four dimensions", *Nucl. Phys. B* **70** (1974) 39, doi:10.1016/0550-3213(74)90355-1.
- [5] A. H. Chamseddine, R. Arnowitt, and P. Nath, "Locally Supersymmetric Grand Unification", *Phys. Rev. Lett.* **49** (1982) 970, doi:10.1103/PhysRevLett.49.970.
- [6] R. Barbieri, S. Ferrara, and C. A. Savoy, "Gauge models with spontaneously broken local supersymmetry", *Phys. Lett. B* **119** (1982) 343, doi:10.1016/0370-2693(82)90685-2.
- [7] L. Hall, J. Lykken, and S. Weinberg, "Supergravity as the messenger of supersymmetry breaking", *Phys. Rev. D* **27** (1983) 2359, doi:10.1103/PhysRevD.27.2359.
- [8] CMS Collaboration, "Search for new physics in the multijet and missing transverse momentum final state in proton-proton collisions at $\sqrt{s} = 8$ TeV", *JHEP* **06** (2014) 055, doi:10.1007/JHEP06(2014)055, arXiv:1402.4770.
- [9] ATLAS Collaboration, "Search for new phenomena in final states with large jet multiplicities and missing transverse momentum at $\sqrt{s} = 8$ TeV proton-proton collisions using the ATLAS experiment", *JHEP* **10** (2013) 130, doi:10.1007/JHEP10(2013)130, arXiv:1308.1841. [Erratum: doi:10.1007/JHEP01(2014)109].
- [10] CMS Collaboration, "Search for new physics in events with same-sign dileptons and jets in pp collisions at $\sqrt{s} = 8$ TeV", *JHEP* **01** (2014) 163, doi:10.1007/JHEP01(2014)163, arXiv:1311.6736. [Erratum: doi:10.1007/JHEP01(2015)014].
- [11] CMS Collaboration, "Search for physics beyond the standard model in events with two leptons, jets, and missing transverse momentum in pp collisions at $\sqrt{s} = 8$ TeV", *JHEP* **04** (2015) 124, doi:10.1007/JHEP04(2015)124, arXiv:1502.06031.
- [12] ATLAS Collaboration, "Search for supersymmetry at $\sqrt{s} = 8$ TeV in final states with jets and two same-sign leptons or three leptons with the ATLAS detector", *JHEP* **06** (2014) 035, doi:10.1007/JHEP06(2014)035, arXiv:1404.2500.
- [13] ATLAS Collaboration, "Search for supersymmetry in events containing a same-flavour opposite-sign dilepton pair, jets, and large missing transverse momentum in $\sqrt{s} = 8$ TeV pp collisions with the ATLAS detector", *Eur. Phys. J. C* **75** (2015) 318, doi:10.1140/epjc/s10052-015-3518-2, arXiv:1503.03290.
- [14] ATLAS Collaboration, "Search for squarks and gluinos with the ATLAS detector in final states with jets and missing transverse momentum using $\sqrt{s} = 8$ TeV proton-proton collision data", *JHEP* **09** (2014) 176, doi:10.1007/JHEP09(2014)176, arXiv:1405.7875.
- [15] CMS Collaboration, "Searches for supersymmetry using the M_{T2} variable in hadronic events produced in pp collisions at 8 TeV", *JHEP* **05** (2015) 078, doi:10.1007/JHEP05(2015)078, arXiv:1502.04358.
- [16] G. R. Farrar and P. Fayet, "Phenomenology of the production, decay, and detection of new hadronic states associated with supersymmetry", *Phys. Lett. B* **76** (1978) 575, doi:10.1016/0370-2693(78)90858-4.

- [17] CMS Collaboration, “Searches for electroweak production of charginos, neutralinos, and sleptons decaying to leptons and W, Z, and Higgs bosons in pp collisions at 8 TeV”, *Eur. Phys. J. C* **74** (2014) 3036, doi:10.1140/epjc/s10052-014-3036-7, arXiv:1405.7570.
- [18] ATLAS Collaboration, “Search for direct production of charginos and neutralinos in events with three leptons and missing transverse momentum in $\sqrt{s} = 8$ TeV pp collisions with the ATLAS detector”, *JHEP* **04** (2014) 169, doi:10.1007/JHEP04(2014)169, arXiv:1402.7029.
- [19] B. Dutta et al., “Vector boson fusion processes as a probe of supersymmetric electroweak sectors at the LHC”, *Phys. Rev. D* **87** (2013) 035029, doi:10.1103/PhysRevD.87.035029, arXiv:1210.0964.
- [20] A. G. Delannoy et al., “Probing Dark Matter at the LHC Using Vector Boson Fusion Processes”, *Phys. Rev. Lett.* **111** (2013) 061801, doi:10.1103/PhysRevLett.111.061801, arXiv:1304.7779.
- [21] CMS Collaboration, “Search for invisible decays of Higgs bosons in the vector boson fusion and associated ZH production modes”, *Eur. Phys. J. C* **74** (2014) 2980, doi:10.1140/epjc/s10052-014-2980-6, arXiv:1404.1344.
- [22] CMS Collaboration, “The CMS experiment at the CERN LHC”, *JINST* **3** (2008) S08004, doi:10.1088/1748-0221/3/08/S08004.
- [23] CMS Collaboration, “Particle-Flow Event Reconstruction in CMS and Performance for Jets, Taus, and E_T^{miss} ”, CMS Physics Analysis Summary CMS-PAS-PFT-09-001, 2009.
- [24] CMS Collaboration, “Commissioning of the Particle-flow Event Reconstruction with the first LHC collisions recorded in the CMS detector”, CMS Physics Analysis Summary CMS-PAS-PFT-10-001, 2010.
- [25] M. Cacciari, G. P. Salam, and G. Soyez, “The anti- k_r jet clustering algorithm”, *JHEP* **04** (2008) 063, doi:10.1088/1126-6708/2008/04/063, arXiv:0802.1189.
- [26] CMS Collaboration, “Pileup Jet Identification”, CMS Physics Analysis Summary CMS-PAS-JME-13-005, 2013.
- [27] CMS Collaboration, “Determination of jet energy calibration and transverse momentum resolution in CMS”, *JINST* **6** (2011) 11002, doi:10.1088/1748-0221/6/11/P11002, arXiv:1107.4277.
- [28] CMS Collaboration, “Identification of b-quark jets with the CMS experiment”, *JINST* **8** (2013) P04013, doi:10.1088/1748-0221/8/04/P04013, arXiv:1211.4462.
- [29] CMS Collaboration, “Performance of b tagging at $\sqrt{s} = 8$ TeV in multijet, $t\bar{t}$ and boosted topology events”, CMS Physics Analysis Summary CMS-PAS-BTV-13-001, 2013.
- [30] CMS Collaboration, “The performance of the CMS muon detector in proton-proton collisions at $\sqrt{s} = 7$ TeV at the LHC”, *JINST* **8** (2013) P11002, doi:10.1088/1748-0221/8/11/P11002, arXiv:1306.6905.
- [31] CMS Collaboration, “Performance of electron reconstruction and selection with the CMS detector in proton-proton collisions at $\sqrt{s} = 8$ TeV”, *JINST* **10** (2015) P06005, doi:10.1088/1748-0221/10/06/P06005, arXiv:1502.02701.

- [32] CMS Collaboration, “Performance of τ -lepton reconstruction and identification in CMS”, *J. Instrum.* **7** (2012) P01001, doi:10.1088/1748-0221/7/01/P01001.
- [33] J. Alwall et al., “MadGraph 5: going beyond”, *JHEP* **06** (2011) 128, doi:10.1007/JHEP06(2011)128, arXiv:1106.0522.
- [34] S. Frixione, P. Nason, and C. Oleari, “Matching NLO QCD computations with parton shower simulations: the POWHEG method”, *JHEP* **11** (2007) 070, doi:10.1088/1126-6708/2007/11/070, arXiv:0709.2092.
- [35] M. Czakon, P. Fiedler, and A. Mitov, “Total Top-Quark Pair-Production Cross Section at Hadron Colliders Through $O(\alpha_s^4)$ ”, *Phys. Rev. Lett.* **110** (2013) 252004, doi:10.1103/PhysRevLett.110.252004, arXiv:1303.6254.
- [36] N. Kidonakis, “Next-to-next-to-leading logarithm resummation for s-channel single top quark production”, *Phys. Rev. D* **81** (2010) 054028, doi:10.1103/PhysRevD.81.054028, arXiv:1001.5034.
- [37] R. Gavin, Y. Li, F. Petriello, and S. Quackenbush, “FEWZ 2.0: A code for hadronic Z production at next-to-next-to-leading order”, *Comput. Phys. Commun.* **182** (2011) 2388, doi:10.1016/j.cpc.2011.06.008, arXiv:1011.3540.
- [38] J. M. Campbell and R. K. Ellis, “MCFM for the Tevatron and the LHC”, *Nucl. Phys. Proc. Suppl.* **205-206** (2010) 10, doi:10.1016/j.nuclphysbps.2010.08.011, arXiv:1007.3492.
- [39] K. Arnold et al., “VBFNLO: A parton level Monte Carlo for processes with electroweak bosons”, *Comput. Phys. Commun.* **180** (2009) 1661, doi:10.1016/j.cpc.2009.03.006, arXiv:0811.4559.
- [40] J. Pumplin et al., “New generation of parton distributions with uncertainties from global QCD analysis”, *JHEP* **07** (2002) 012, doi:10.1088/1126-6708/2002/07/012, arXiv:hep-ph/0201195.
- [41] P. M. Nadolsky et al., “Implications of CTEQ global analysis for collider observables”, *Phys. Rev. D* **78** (2008) 013004, doi:10.1103/PhysRevD.78.013004, arXiv:0802.0007.
- [42] T. Sjöstrand, S. Mrenna, and P. Z. Skands, “PYTHIA 6.4 physics and manual”, *JHEP* **05** (2006) 026, doi:10.1088/1126-6708/2006/05/026, arXiv:hep-ph/0603175.
- [43] N. Davidson, G. Nanava, and Z. W. T. Przedziński, E. Richter-Wąs, “Universal Interface of TAUOLA Technical and Physics Documentation”, *Comput. Phys. Commun.* **183** (2012) 821, doi:10.1016/j.cpc.2011.12.009, arXiv:1002.0543.
- [44] GEANT4 Collaboration, “GEANT4—a simulation toolkit”, *Nucl. Instrum. Meth. A* **506** (2003) 250, doi:10.1016/S0168-9002(03)01368-8.
- [45] S. Abdullin et al., “The fast simulation of the CMS detector at LHC”, *J. Phys. Conf. Ser.* **331** (2011) 032049, doi:10.1088/1742-6596/331/3/032049.
- [46] CMS Collaboration, “Measurement of the inclusive Z cross section via decays to tau pairs in pp collisions at $\sqrt{s} = 7$ TeV”, *J. High Energy Phys.* **08** (2011) 117, doi:10.1007/JHEP08(2011)117.

- [47] CMS Collaboration, “CMS Luminosity Based on Pixel Cluster Counting - Summer 2013 Update”, CMS Physics Analysis Summary CMS-PAS-LUM-13-001, 2013.
- [48] S. Alekhin et al., “The PDF4LHC Working Group Interim Report”, (2011).
arXiv:1101.0536.
- [49] M. Botje et al., “The PDF4LHC Working Group Interim Recommendations”, (2011).
arXiv:1101.0538.
- [50] A. D. Martin, W. J. Stirling, R. S. Thorne, and G. Watt, “Update of parton distributions at NNLO”, *Phys. Lett. B* **652** (2007) 292, doi:10.1016/j.physletb.2007.07.040,
arXiv:0706.0459.
- [51] M. Ubiali, “NNPDF1.0 parton set for the LHC”, *Nucl. Phys. Proc. Suppl.* **186** (2009) 62,
doi:10.1016/j.nuclphysbps.2008.12.020, arXiv:0809.3716.
- [52] A. L. Read, “Presentation of search results: the CL_s technique”, *J. Phys. G* **28** (2002) 2693,
doi:10.1088/0954-3899/28/10/313.
- [53] T. Junk, “Confidence level computation for combining searches with small statistics”,
Nucl. Instrum. Meth. A **434** (1999) 435, doi:10.1016/S0168-9002(99)00498-2.
- [54] G. Cowan, K. Cranmer, E. Gross, and O. Vitells, “Asymptotic formulae for likelihood-based tests of new physics”, *Eur. Phys. J. C* **71** (2011) 1554,
doi:10.1140/epjc/s10052-011-1554-0, arXiv:1007.1727. [Erratum:
doi:10.1140/epjc/s10052-013-2501-z].

A The CMS Collaboration

Yerevan Physics Institute, Yerevan, Armenia

V. Khachatryan, A.M. Sirunyan, A. Tumasyan

Institut für Hochenergiephysik der OeAW, Wien, Austria

W. Adam, E. Asilar, T. Bergauer, J. Brandstetter, E. Brondolin, M. Dragicevic, J. Erö, M. Flechl, M. Friedl, R. Frühwirth¹, V.M. Ghete, C. Hartl, N. Hörmann, J. Hrubec, M. Jeitler¹, V. Knünz, A. König, M. Krammer¹, I. Krätschmer, D. Liko, T. Matsushita, I. Mikulec, D. Rabady², B. Rahbaran, H. Rohringer, J. Schieck¹, R. Schöfbeck, J. Strauss, W. Treberer-Treberspurg, W. Waltenberger, C.-E. Wulz¹

National Centre for Particle and High Energy Physics, Minsk, Belarus

V. Mossolov, N. Shumeiko, J. Suarez Gonzalez

Universiteit Antwerpen, Antwerpen, Belgium

S. Alderweireldt, T. Cornelis, E.A. De Wolf, X. Janssen, A. Knutsson, J. Lauwers, S. Luyckx, S. Ochesanu, R. Rougny, M. Van De Klundert, H. Van Haevermaet, P. Van Mechelen, N. Van Remortel, A. Van Spilbeeck

Vrije Universiteit Brussel, Brussel, Belgium

S. Abu Zeid, F. Blekman, J. D'Hondt, N. Daci, I. De Bruyn, K. Deroover, N. Heracleous, J. Keaveney, S. Lowette, L. Moreels, A. Olbrechts, Q. Python, D. Strom, S. Tavernier, W. Van Doninck, P. Van Mulders, G.P. Van Onsem, I. Van Parijs

Université Libre de Bruxelles, Bruxelles, Belgium

P. Barria, C. Caillol, B. Clerboux, G. De Lentdecker, H. Delannoy, G. Fasanella, L. Favart, A.P.R. Gay, A. Grebenyuk, G. Karapostoli, T. Lenzi, A. Léonard, T. Maerschalk, A. Marinov, L. Perniè, A. Randle-conde, T. Reis, T. Seva, C. Vander Velde, P. Vanlaer, R. Yonamine, F. Zenoni, F. Zhang³

Ghent University, Ghent, Belgium

K. Beernaert, L. Benucci, A. Cimmino, S. Crucy, D. Dobur, A. Fagot, G. Garcia, M. Gul, J. Mccartin, A.A. Ocampo Rios, D. Poyraz, D. Ryckbosch, S. Salva, M. Sigamani, N. Strobbe, M. Tytgat, W. Van Driessche, E. Yazgan, N. Zaganidis

Université Catholique de Louvain, Louvain-la-Neuve, Belgium

S. Basegmez, C. Beluffi⁴, O. Bondu, S. Brochet, G. Bruno, R. Castello, A. Caudron, L. Ceard, G.G. Da Silveira, C. Delaere, D. Favart, L. Forthomme, A. Giammanco⁵, J. Hollar, A. Jafari, P. Jez, M. Komm, V. Lemaitre, A. Mertens, C. Nuttens, L. Perrini, A. Pin, K. Piotrkowski, A. Popov⁶, L. Quertenmont, M. Selvaggi, M. Vidal Marono

Université de Mons, Mons, Belgium

N. Belyi, G.H. Hammad

Centro Brasileiro de Pesquisas Fisicas, Rio de Janeiro, Brazil

W.L. Aldá Júnior, G.A. Alves, L. Brito, M. Correa Martins Junior, M. Hamer, C. Hensel, C. Mora Herrera, A. Moraes, M.E. Pol, P. Rebello Teles

Universidade do Estado do Rio de Janeiro, Rio de Janeiro, Brazil

E. Belchior Batista Das Chagas, W. Carvalho, J. Chinellato⁷, A. Custódio, E.M. Da Costa, D. De Jesus Damiao, C. De Oliveira Martins, S. Fonseca De Souza, L.M. Huertas Guativa, H. Malbouisson, D. Matos Figueiredo, L. Mundim, H. Nogima, W.L. Prado Da Silva, A. Santoro, A. Sznajder, E.J. Tonelli Manganote⁷, A. Vilela Pereira

Universidade Estadual Paulista ^a, Universidade Federal do ABC ^b, São Paulo, Brazil

S. Ahuja^a, C.A. Bernardes^b, A. De Souza Santos^b, S. Dogra^a, T.R. Fernandez Perez Tomei^a, E.M. Gregores^b, P.G. Mercadante^b, C.S. Moon^{a,8}, S.F. Novaes^a, Sandra S. Padula^a, D. Romero Abad, J.C. Ruiz Vargas

Institute for Nuclear Research and Nuclear Energy, Sofia, Bulgaria

A. Aleksandrov, V. Genchev[†], R. Hadjiiska, P. Iaydjiev, M. Rodozov, S. Stoykova, G. Sultanov, M. Vutova

University of Sofia, Sofia, Bulgaria

A. Dimitrov, I. Glushkov, L. Litov, B. Pavlov, P. Petkov

Institute of High Energy Physics, Beijing, China

M. Ahmad, J.G. Bian, G.M. Chen, H.S. Chen, M. Chen, T. Cheng, R. Du, C.H. Jiang, R. Plestina⁹, F. Romeo, S.M. Shaheen, J. Tao, C. Wang, Z. Wang, H. Zhang

State Key Laboratory of Nuclear Physics and Technology, Peking University, Beijing, China

C. Asawatrangkuldee, Y. Ban, Q. Li, S. Liu, Y. Mao, S.J. Qian, D. Wang, Z. Xu, W. Zou

Universidad de Los Andes, Bogota, Colombia

C. Avila, A. Cabrera, L.F. Chaparro Sierra, C. Florez, J.P. Gomez, B. Gomez Moreno, J.C. Sanabria

University of Split, Faculty of Electrical Engineering, Mechanical Engineering and Naval Architecture, Split, Croatia

N. Godinovic, D. Lelas, D. Polic, I. Puljak, P.M. Ribeiro Cipriano

University of Split, Faculty of Science, Split, Croatia

Z. Antunovic, M. Kovac

Institute Rudjer Boskovic, Zagreb, Croatia

V. Brigljevic, K. Kadija, J. Luetic, S. Micanovic, L. Sudic

University of Cyprus, Nicosia, Cyprus

A. Attikis, G. Mavromanolakis, J. Mousa, C. Nicolaou, F. Ptochos, P.A. Razis, H. Rykaczewski

Charles University, Prague, Czech Republic

M. Bodlak, M. Finger¹⁰, M. Finger Jr.¹⁰

Academy of Scientific Research and Technology of the Arab Republic of Egypt, Egyptian Network of High Energy Physics, Cairo, Egypt

A.A. Abdelalim^{11,12}, A. Awad^{13,14}, A. Mahrous¹², A. Radi^{14,13}

National Institute of Chemical Physics and Biophysics, Tallinn, Estonia

B. Calpas, M. Kadastik, M. Murumaa, M. Raidal, A. Tiko, C. Veelken

Department of Physics, University of Helsinki, Helsinki, Finland

P. Eerola, J. Pekkanen, M. Voutilainen

Helsinki Institute of Physics, Helsinki, Finland

J. Härkönen, V. Karimäki, R. Kinnunen, T. Lampén, K. Lassila-Perini, S. Lehti, T. Lindén, P. Luukka, T. Mäenpää, T. Peltola, E. Tuominen, J. Tuominiemi, E. Tuovinen, L. Wendland

Lappeenranta University of Technology, Lappeenranta, Finland

J. Talvitie, T. Tuuva

DSM/IRFU, CEA/Saclay, Gif-sur-Yvette, France

M. Besancon, F. Couderc, M. Dejardin, D. Denegri, B. Fabbro, J.L. Faure, C. Favaro, F. Ferri, S. Ganjour, A. Givernaud, P. Gras, G. Hamel de Monchenault, P. Jarry, E. Locci, M. Machet, J. Malcles, J. Rander, A. Rosowsky, M. Titov, A. Zghiche

Laboratoire Leprince-Ringuet, Ecole Polytechnique, IN2P3-CNRS, Palaiseau, France

I. Antropov, S. Baffioni, F. Beaudette, P. Busson, L. Cadamuro, E. Chapon, C. Charlot, T. Dahms, O. Davignon, N. Filipovic, A. Florent, R. Granier de Cassagnac, S. Lisniak, L. Mastrolorenzo, P. Miné, I.N. Naranjo, M. Nguyen, C. Ochando, G. Ortona, P. Paganini, S. Regnard, R. Salerno, J.B. Sauvan, Y. Sirois, T. Strebler, Y. Yilmaz, A. Zabi

Institut Pluridisciplinaire Hubert Curien, Université de Strasbourg, Université de Haute Alsace Mulhouse, CNRS/IN2P3, Strasbourg, France

J.-L. Agram¹⁵, J. Andrea, A. Aubin, D. Bloch, J.-M. Brom, M. Buttignol, E.C. Chabert, N. Chanon, C. Collard, E. Conte¹⁵, X. Coubez, J.-C. Fontaine¹⁵, D. Gelé, U. Goerlach, C. Goetzmann, A.-C. Le Bihan, J.A. Merlin², K. Skovpen, P. Van Hove

Centre de Calcul de l'Institut National de Physique Nucleaire et de Physique des Particules, CNRS/IN2P3, Villeurbanne, France

S. Gadrat

Université de Lyon, Université Claude Bernard Lyon 1, CNRS-IN2P3, Institut de Physique Nucléaire de Lyon, Villeurbanne, France

S. Beauceron, C. Bernet, G. Boudoul, E. Bouvier, C.A. Carrillo Montoya, J. Chasserat, R. Chierici, D. Contardo, B. Courbon, P. Depasse, H. El Mamouni, J. Fan, J. Fay, S. Gascon, M. Gouzevitch, B. Ille, F. Lagarde, I.B. Laktineh, M. Lethuillier, L. Mirabito, A.L. Pequegnot, S. Perries, J.D. Ruiz Alvarez, D. Sabes, L. Sgandurra, V. Sordini, M. Vander Donckt, P. Verdier, S. Viret, H. Xiao

Georgian Technical University, Tbilisi, Georgia

T. Toriashvili¹⁶

Tbilisi State University, Tbilisi, Georgia

Z. Tsamalaidze¹⁰

RWTH Aachen University, I. Physikalisches Institut, Aachen, Germany

C. Autermann, S. Beranek, M. Edelhoff, L. Feld, A. Heister, M.K. Kiesel, K. Klein, M. Lipinski, A. Ostapchuk, M. Preuten, F. Raupach, S. Schael, J.F. Schulte, T. Verlage, H. Weber, B. Wittmer, V. Zhukov⁶

RWTH Aachen University, III. Physikalisches Institut A, Aachen, Germany

M. Ata, M. Brodski, E. Dietz-Laursonn, D. Duchardt, M. Endres, M. Erdmann, S. Erdweg, T. Esch, R. Fischer, A. Güth, T. Hebbeker, C. Heidemann, K. Hoepfner, D. Klingebiel, S. Knutzen, P. Kreuzer, M. Merschmeyer, A. Meyer, P. Millet, M. Olschewski, K. Padeken, P. Papacz, T. Pook, M. Radziej, H. Reithler, M. Rieger, F. Scheuch, L. Sonnenschein, D. Teyssier, S. Thüer

RWTH Aachen University, III. Physikalisches Institut B, Aachen, Germany

V. Cherepanov, Y. Erdogan, G. Flügge, H. Geenen, M. Geisler, F. Hoehle, B. Kargoll, T. Kress, Y. Kuessel, A. Künsken, J. Lingemann², A. Nehr Korn, A. Nowack, I.M. Nugent, C. Pistone, O. Pooth, A. Stahl

Deutsches Elektronen-Synchrotron, Hamburg, Germany

M. Aldaya Martin, I. Asin, N. Bartosik, O. Behnke, U. Behrens, A.J. Bell, K. Borras, A. Burgmeier, A. Cakir, L. Calligaris, A. Campbell, S. Choudhury, F. Costanza, C. Diez

Pardos, G. Dolinska, S. Dooling, T. Dorland, G. Eckerlin, D. Eckstein, T. Eichhorn, G. Flucke, E. Gallo, J. Garay Garcia, A. Geiser, A. Gizhko, P. Gunnellini, J. Hauk, M. Hempel¹⁷, H. Jung, A. Kalogeropoulos, O. Karacheban¹⁷, M. Kasemann, P. Katsas, J. Kieseler, C. Kleinwort, I. Korol, W. Lange, J. Leonard, K. Lipka, A. Lobanov, W. Lohmann¹⁷, R. Mankel, I. Marfin¹⁷, I.-A. Melzer-Pellmann, A.B. Meyer, G. Mittag, J. Mnich, A. Mussgiller, S. Naumann-Emme, A. Nayak, E. Ntomari, H. Perrey, D. Pitzl, R. Placakyte, A. Raspereza, B. Roland, M.Ö. Sahin, P. Saxena, T. Schoerner-Sadenius, M. Schröder, C. Seitz, S. Spannagel, K.D. Trippkewitz, R. Walsh, C. Wissing

University of Hamburg, Hamburg, Germany

V. Blobel, M. Centis Vignali, A.R. Draeger, J. Erfle, E. Garutti, K. Goebel, D. Gonzalez, M. Görner, J. Haller, M. Hoffmann, R.S. Höing, A. Junkes, R. Klanner, R. Kogler, T. Lapsien, T. Lenz, I. Marchesini, D. Marconi, M. Meyer, D. Nowatschin, J. Ott, F. Pantaleo², T. Peiffer, A. Perieanu, N. Pietsch, J. Poehlsen, D. Rathjens, C. Sander, H. Schettler, P. Schleper, E. Schlieckau, A. Schmidt, J. Schwandt, M. Seidel, V. Sola, H. Stadie, G. Steinbrück, H. Tholen, D. Troendle, E. Usai, L. Vanelderen, A. Vanhoefer, B. Vormwald

Institut für Experimentelle Kernphysik, Karlsruhe, Germany

M. Akbiyik, C. Barth, C. Baus, J. Berger, C. Böser, E. Butz, T. Chwalek, F. Colombo, W. De Boer, A. Descroix, A. Dierlamm, S. Fink, F. Frensch, M. Giffels, A. Gilbert, F. Hartmann², S.M. Heindl, U. Husemann, I. Katkov⁶, A. Kornmayer², P. Lobelle Pardo, B. Maier, H. Mildner, M.U. Mozer, T. Müller, Th. Müller, M. Plagge, G. Quast, K. Rabbertz, S. Röcker, F. Roscher, H.J. Simonis, F.M. Stober, R. Ulrich, J. Wagner-Kuhr, S. Wayand, M. Weber, T. Weiler, C. Wöhrmann, R. Wolf

Institute of Nuclear and Particle Physics (INPP), NCSR Demokritos, Aghia Paraskevi, Greece

G. Anagnostou, G. Daskalakis, T. Gerasis, V.A. Giakoumopoulou, A. Kyriakis, D. Loukas, A. Psallidas, I. Topsis-Giotis

University of Athens, Athens, Greece

A. Agapitos, S. Kesisoglou, A. Panagiotou, N. Saoulidou, E. Tziaferi

University of Ioánnina, Ioánnina, Greece

I. Evangelou, G. Flouris, C. Foudas, P. Kokkas, N. Loukas, N. Manthos, I. Papadopoulos, E. Paradas, J. Strologas

Wigner Research Centre for Physics, Budapest, Hungary

G. Bencze, C. Hajdu, A. Hazi, P. Hidas, D. Horvath¹⁸, F. Sikler, V. Veszpremi, G. Vesztergombi¹⁹, A.J. Zsigmond

Institute of Nuclear Research ATOMKI, Debrecen, Hungary

N. Beni, S. Czellar, J. Karancsi²⁰, J. Molnar, Z. Szillasi

University of Debrecen, Debrecen, Hungary

M. Bartók²¹, A. Makovec, P. Raics, Z.L. Trocsanyi, B. Ujvari

National Institute of Science Education and Research, Bhubaneswar, India

P. Mal, K. Mandal, N. Sahoo, S.K. Swain

Panjab University, Chandigarh, India

S. Bansal, S.B. Beri, V. Bhatnagar, R. Chawla, R. Gupta, U. Bhawandeep, A.K. Kalsi, A. Kaur, M. Kaur, R. Kumar, A. Mehta, M. Mittal, J.B. Singh, G. Walia

University of Delhi, Delhi, India

Ashok Kumar, Arun Kumar, A. Bhardwaj, B.C. Choudhary, R.B. Garg, A. Kumar, S. Malhotra, M. Naimuddin, N. Nishu, K. Ranjan, R. Sharma, V. Sharma

Saha Institute of Nuclear Physics, Kolkata, India

S. Banerjee, S. Bhattacharya, K. Chatterjee, S. Dey, S. Dutta, Sa. Jain, N. Majumdar, A. Modak, K. Mondal, S. Mukherjee, S. Mukhopadhyay, A. Roy, D. Roy, S. Roy Chowdhury, S. Sarkar, M. Sharan

Bhabha Atomic Research Centre, Mumbai, India

A. Abdulsalam, R. Chudasama, D. Dutta, V. Jha, V. Kumar, A.K. Mohanty², L.M. Pant, P. Shukla, A. Topkar

Tata Institute of Fundamental Research, Mumbai, India

T. Aziz, S. Banerjee, S. Bhowmik²², R.M. Chatterjee, R.K. Dewanjee, S. Dugad, S. Ganguly, S. Ghosh, M. Guchait, A. Gurtu²³, G. Kole, S. Kumar, B. Mahakud, M. Maity²², G. Majumder, K. Mazumdar, S. Mitra, G.B. Mohanty, B. Parida, T. Sarkar²², K. Sudhakar, N. Sur, B. Sutar, N. Wickramage²⁴

Indian Institute of Science Education and Research (IISER), Pune, India

S. Chauhan, S. Dube, S. Sharma

Institute for Research in Fundamental Sciences (IPM), Tehran, Iran

H. Bakhshiansohi, H. Behnamian, S.M. Etesami²⁵, A. Fahim²⁶, R. Goldouzian, M. Khakzad, M. Mohammadi Najafabadi, M. Naseri, S. Paktinat Mehdiabadi, F. Rezaei Hosseinabadi, B. Safarzadeh²⁷, M. Zeinali

University College Dublin, Dublin, Ireland

M. Felcini, M. Grunewald

INFN Sezione di Bari ^a, Università di Bari ^b, Politecnico di Bari ^c, Bari, Italy

M. Abbrescia^{a,b}, C. Calabria^{a,b}, C. Caputo^{a,b}, S.S. Chhibra^{a,b}, A. Colaleo^a, D. Creanza^{a,c}, L. Cristella^{a,b}, N. De Filippis^{a,c}, M. De Palma^{a,b}, L. Fiore^a, G. Iaselli^{a,c}, G. Maggi^{a,c}, M. Maggi^a, G. Miniello^{a,b}, S. My^{a,c}, S. Nuzzo^{a,b}, A. Pompili^{a,b}, G. Pugliese^{a,c}, R. Radogna^{a,b}, A. Ranieri^a, G. Selvaggi^{a,b}, L. Silvestris^{a,2}, R. Venditti^{a,b}, P. Verwilligen^a

INFN Sezione di Bologna ^a, Università di Bologna ^b, Bologna, Italy

G. Abbiendi^a, C. Battilana², A.C. Benvenuti^a, D. Bonacorsi^{a,b}, S. Braibant-Giacomelli^{a,b}, L. Brigliadori^{a,b}, R. Campanini^{a,b}, P. Capiluppi^{a,b}, A. Castro^{a,b}, F.R. Cavallo^a, G. Codispoti^{a,b}, M. Cuffiani^{a,b}, G.M. Dallavalle^a, F. Fabbri^a, A. Fanfani^{a,b}, D. Fasanella^{a,b}, P. Giacomelli^a, C. Grandi^a, L. Guiducci^{a,b}, S. Marcellini^a, G. Masetti^a, A. Montanari^a, F.L. Navarria^{a,b}, A. Perrotta^a, A.M. Rossi^{a,b}, T. Rovelli^{a,b}, G.P. Siroli^{a,b}, N. Tosi^{a,b}, R. Travaglini^{a,b}

INFN Sezione di Catania ^a, Università di Catania ^b, CSFNSM ^c, Catania, Italy

G. Cappello^a, M. Chiorboli^{a,b}, S. Costa^{a,b}, F. Giordano^{a,c}, R. Potenza^{a,b}, A. Tricomi^{a,b}, C. Tuve^{a,b}

INFN Sezione di Firenze ^a, Università di Firenze ^b, Firenze, Italy

G. Barbagli^a, V. Ciulli^{a,b}, C. Civinini^a, R. D'Alessandro^{a,b}, E. Focardi^{a,b}, S. Gonzi^{a,b}, V. Gori^{a,b}, P. Lenzi^{a,b}, M. Meschini^a, S. Paoletti^a, G. Sguazzoni^a, A. Tropiano^{a,b}, L. Viliani^{a,b}

INFN Laboratori Nazionali di Frascati, Frascati, Italy

L. Benussi, S. Bianco, F. Fabbri, D. Piccolo

INFN Sezione di Genova ^a, Università di Genova ^b, Genova, Italy

V. Calvelli^{a,b}, F. Ferro^a, M. Lo Vetere^{a,b}, M.R. Monge^{a,b}, E. Robutti^a, S. Tosi^{a,b}

INFN Sezione di Milano-Bicocca ^a, Università di Milano-Bicocca ^b, Milano, Italy

L. Brianza, M.E. Dinardo^{a,b}, S. Fiorendi^{a,b}, S. Gennai^a, R. Gerosa^{a,b}, A. Ghezzi^{a,b}, P. Govoni^{a,b}, S. Malvezzi^a, R.A. Manzoni^{a,b}, B. Marzocchi^{a,b,2}, D. Menasce^a, L. Moroni^a, M. Paganoni^{a,b}, D. Pedrini^a, S. Ragazzi^{a,b}, N. Redaelli^a, T. Tabarelli de Fatis^{a,b}

INFN Sezione di Napoli ^a, Università di Napoli 'Federico II' ^b, Napoli, Italy, Università della Basilicata ^c, Potenza, Italy, Università G. Marconi ^d, Roma, Italy

S. Buontempo^a, N. Cavallo^{a,c}, S. Di Guida^{a,d,2}, M. Esposito^{a,b}, F. Fabozzi^{a,c}, A.O.M. Iorio^{a,b}, G. Lanza^a, L. Lista^a, S. Meola^{a,d,2}, M. Merola^a, P. Paolucci^{a,2}, C. Sciacca^{a,b}, F. Thyssen

INFN Sezione di Padova ^a, Università di Padova ^b, Padova, Italy, Università di Trento ^c, Trento, Italy

P. Azzi^{a,2}, N. Bacchetta^a, L. Benato^{a,b}, D. Bisello^{a,b}, A. Boletti^{a,b}, R. Carlin^{a,b}, A. Carvalho Antunes De Oliveira^{a,b}, P. Checchia^a, M. Dall'Osso^{a,b,2}, T. Dorigo^a, U. Dosselli^a, F. Gasparini^{a,b}, U. Gasparini^{a,b}, F. Gonella^a, A. Gozzelino^a, S. Lacaprara^a, M. Margoni^{a,b}, A.T. Meneguzzo^{a,b}, F. Montecassiano^a, J. Pazzini^{a,b}, N. Pozzobon^{a,b}, P. Ronchese^{a,b}, F. Simonetto^{a,b}, E. Torassa^a, M. Tosi^{a,b}, M. Zanetti, P. Zotto^{a,b}, A. Zucchetta^{a,b,2}, G. Zumerle^{a,b}

INFN Sezione di Pavia ^a, Università di Pavia ^b, Pavia, Italy

A. Braghieri^a, A. Magnani^a, P. Montagna^{a,b}, S.P. Ratti^{a,b}, V. Re^a, C. Riccardi^{a,b}, P. Salvini^a, I. Vai^a, P. Vitulo^{a,b}

INFN Sezione di Perugia ^a, Università di Perugia ^b, Perugia, Italy

L. Alunni Solestizi^{a,b}, M. Biasini^{a,b}, G.M. Bilei^a, D. Ciangottini^{a,b,2}, L. Fanò^{a,b}, P. Lariccia^{a,b}, G. Mantovani^{a,b}, M. Menichelli^a, A. Saha^a, A. Santocchia^{a,b}, A. Spiezia^{a,b}

INFN Sezione di Pisa ^a, Università di Pisa ^b, Scuola Normale Superiore di Pisa ^c, Pisa, Italy

K. Androsov^{a,28}, P. Azzurri^a, G. Bagliesi^a, J. Bernardini^a, T. Boccali^a, G. Broccolo^{a,c}, R. Castaldi^a, M.A. Ciocci^{a,28}, R. Dell'Orso^a, S. Donato^{a,c,2}, G. Fedi, L. Foà^{a,c†}, A. Giassi^a, M.T. Grippo^{a,28}, F. Ligabue^{a,c}, T. Lomtadze^a, L. Martini^{a,b}, A. Messineo^{a,b}, F. Palla^a, A. Rizzi^{a,b}, A. Savoy-Navarro^{a,29}, A.T. Serban^a, P. Spagnolo^a, P. Squillacioti^{a,28}, R. Tenchini^a, G. Tonelli^{a,b}, A. Venturi^a, P.G. Verdini^a

INFN Sezione di Roma ^a, Università di Roma ^b, Roma, Italy

L. Barone^{a,b}, F. Cavallari^a, G. D'imperio^{a,b,2}, D. Del Re^{a,b}, M. Diemoz^a, S. Gelli^{a,b}, C. Jorda^a, E. Longo^{a,b}, F. Margaroli^{a,b}, P. Meridiani^a, F. Micheli^{a,b}, G. Organtini^{a,b}, R. Paramatti^a, F. Preiato^{a,b}, S. Rahatlou^{a,b}, C. Rovelli^a, F. Santanastasio^{a,b}, P. Traczyk^{a,b,2}

INFN Sezione di Torino ^a, Università di Torino ^b, Torino, Italy, Università del Piemonte Orientale ^c, Novara, Italy

N. Amapane^{a,b}, R. Arcidiacono^{a,c,2}, S. Argiro^{a,b}, M. Arneodo^{a,c}, R. Bellan^{a,b}, C. Biino^a, N. Cartiglia^a, M. Costa^{a,b}, R. Covarelli^{a,b}, A. Degano^{a,b}, G. Dellacasa^a, N. Demaria^a, L. Finco^{a,b,2}, B. Kiani^{a,b}, C. Mariotti^a, S. Maselli^a, E. Migliore^{a,b}, V. Monaco^{a,b}, E. Monteil^{a,b}, M. Musich^a, M.M. Obertino^{a,b}, L. Pacher^{a,b}, N. Pastrone^a, M. Pelliccioni^a, G.L. Pinna Angioni^{a,b}, F. Ravera^{a,b}, A. Romero^{a,b}, M. Ruspa^{a,c}, R. Sacchi^{a,b}, A. Solano^{a,b}, A. Staiano^a

INFN Sezione di Trieste ^a, Università di Trieste ^b, Trieste, Italy

S. Belforte^a, V. Candelise^{a,b,2}, M. Casarsa^a, F. Cossutti^a, G. Della Ricca^{a,b}, B. Gobbo^a, C. La Licata^{a,b}, M. Marone^{a,b}, A. Schizzi^{a,b}, T. Umer^{a,b}, A. Zanetti^a

Kangwon National University, Chunchon, Korea

S. Chang, A. Kropivnitskaya, S.K. Nam

Kyungpook National University, Daegu, Korea

D.H. Kim, G.N. Kim, M.S. Kim, D.J. Kong, S. Lee, Y.D. Oh, A. Sakharov, D.C. Son

Chonbuk National University, Jeonju, Korea

J.A. Brochero Cifuentes, H. Kim, T.J. Kim, M.S. Ryu

Chonnam National University, Institute for Universe and Elementary Particles, Kwangju, Korea

S. Song

Korea University, Seoul, Korea

S. Choi, Y. Go, D. Gyun, B. Hong, M. Jo, H. Kim, Y. Kim, B. Lee, K. Lee, K.S. Lee, S. Lee, S.K. Park, Y. Roh

Seoul National University, Seoul, Korea

H.D. Yoo

University of Seoul, Seoul, Korea

M. Choi, H. Kim, J.H. Kim, J.S.H. Lee, I.C. Park, G. Ryu

Sungkyunkwan University, Suwon, Korea

Y. Choi, Y.K. Choi, J. Goh, D. Kim, E. Kwon, J. Lee, I. Yu

Vilnius University, Vilnius, Lithuania

A. Juodagalvis, J. Vaitkus

National Centre for Particle Physics, Universiti Malaya, Kuala Lumpur, Malaysia

I. Ahmed, Z.A. Ibrahim, J.R. Komaragiri, M.A.B. Md Ali³⁰, F. Mohamad Idris³¹, W.A.T. Wan Abdullah, M.N. Yusli

Centro de Investigacion y de Estudios Avanzados del IPN, Mexico City, Mexico

E. Casimiro Linares, H. Castilla-Valdez, E. De La Cruz-Burelo, I. Heredia-de La Cruz³², A. Hernandez-Almada, R. Lopez-Fernandez, A. Sanchez-Hernandez

Universidad Iberoamericana, Mexico City, Mexico

S. Carrillo Moreno, F. Vazquez Valencia

Benemerita Universidad Autonoma de Puebla, Puebla, Mexico

I. Pedraza, H.A. Salazar Ibarguen

Universidad Autónoma de San Luis Potosí, San Luis Potosí, Mexico

A. Morelos Pineda

University of Auckland, Auckland, New Zealand

D. Krofcheck

University of Canterbury, Christchurch, New Zealand

P.H. Butler, S. Reucroft

National Centre for Physics, Quaid-I-Azam University, Islamabad, Pakistan

A. Ahmad, M. Ahmad, Q. Hassan, H.R. Hoorani, W.A. Khan, T. Khurshid, M. Shoaib

National Centre for Nuclear Research, Swierk, Poland

H. Bialkowska, M. Bluj, B. Boimska, T. Frueboes, M. Górski, M. Kazana, K. Nawrocki, K. Romanowska-Rybinska, M. Szleper, P. Zalewski

Institute of Experimental Physics, Faculty of Physics, University of Warsaw, Warsaw, Poland
G. Brona, K. Bunkowski, K. Doroba, A. Kalinowski, M. Konecki, J. Krolikowski, M. Misiura, M. Olszewski, M. Walczak

Laboratório de Instrumentação e Física Experimental de Partículas, Lisboa, Portugal
P. Bargassa, C. Beirão Da Cruz E Silva, A. Di Francesco, P. Faccioli, P.G. Ferreira Parracho, M. Gallinaro, N. Leonardo, L. Lloret Iglesias, F. Nguyen, J. Rodrigues Antunes, J. Seixas, O. Toldaiev, D. Vadrucio, J. Varela, P. Vischia

Joint Institute for Nuclear Research, Dubna, Russia
S. Afanasiev, P. Bunin, M. Gavrilenko, I. Golutvin, I. Gorbunov, A. Kamenev, V. Karjavin, V. Konoplyanikov, A. Lanev, A. Malakhov, V. Matveev³³, P. Moiseenz, V. Palichik, V. Perelygin, S. Shmatov, S. Shulha, N. Skatchkov, V. Smirnov, A. Zarubin

Petersburg Nuclear Physics Institute, Gatchina (St. Petersburg), Russia
V. Golovtsov, Y. Ivanov, V. Kim³⁴, E. Kuznetsova, P. Levchenko, V. Murzin, V. Oreshkin, I. Smirnov, V. Sulimov, L. Uvarov, S. Vavilov, A. Vorobyev

Institute for Nuclear Research, Moscow, Russia
Yu. Andreev, A. Dermenev, S. Gninenko, N. Golubev, A. Karneyeu, M. Kirsanov, N. Krasnikov, A. Pashenkov, D. Tlisov, A. Toropin

Institute for Theoretical and Experimental Physics, Moscow, Russia
V. Epshteyn, V. Gavrillov, N. Lychkovskaya, V. Popov, I. Pozdnyakov, G. Safronov, A. Spiridonov, E. Vlasov, A. Zhokin

National Research Nuclear University 'Moscow Engineering Physics Institute' (MEPhI), Moscow, Russia
A. Bylinkin

P.N. Lebedev Physical Institute, Moscow, Russia
V. Andreev, M. Azarkin³⁵, I. Dremin³⁵, M. Kirakosyan, A. Leonidov³⁵, G. Mesyats, S.V. Rusakov, A. Vinogradov

Skobeltsyn Institute of Nuclear Physics, Lomonosov Moscow State University, Moscow, Russia
A. Baskakov, A. Belyaev, E. Boos, M. Dubinin³⁶, L. Dudko, A. Ershov, A. Gribushin, V. Klyukhin, O. Kodolova, I. Lokhtin, I. Myagkov, S. Obraztsov, S. Petrushanko, V. Savrin, A. Snigirev

State Research Center of Russian Federation, Institute for High Energy Physics, Protvino, Russia
I. Azhgirey, I. Bayshev, S. Bitioukov, V. Kachanov, A. Kalinin, D. Konstantinov, V. Krychkin, V. Petrov, R. Ryutin, A. Sobol, L. Tourtchanovitch, S. Troshin, N. Tyurin, A. Uzunian, A. Volkov

University of Belgrade, Faculty of Physics and Vinca Institute of Nuclear Sciences, Belgrade, Serbia
P. Adzic³⁷, M. Ekmedzic, J. Milosevic, V. Rekovic

Centro de Investigaciones Energéticas Medioambientales y Tecnológicas (CIEMAT), Madrid, Spain
J. Alcaraz Maestre, E. Calvo, M. Cerrada, M. Chamizo Llatas, N. Colino, B. De La Cruz, A. Delgado Peris, D. Domínguez Vázquez, A. Escalante Del Valle, C. Fernandez Bedoya, J.P. Fernández Ramos, J. Flix, M.C. Fouz, P. Garcia-Abia, O. Gonzalez Lopez, S. Goy Lopez,

J.M. Hernandez, M.I. Josa, E. Navarro De Martino, A. Pérez-Calero Yzquierdo, J. Puerta Pelayo, A. Quintario Olmeda, I. Redondo, L. Romero, M.S. Soares

Universidad Autónoma de Madrid, Madrid, Spain

C. Albajar, J.F. de Trocóniz, M. Missiroli, D. Moran

Universidad de Oviedo, Oviedo, Spain

H. Brun, J. Cuevas, J. Fernandez Menendez, S. Folgueras, I. Gonzalez Caballero, E. Palencia Cortezon, J.M. Vizan Garcia

Instituto de Física de Cantabria (IFCA), CSIC-Universidad de Cantabria, Santander, Spain

I.J. Cabrillo, A. Calderon, J.R. Castiñeiras De Saa, P. De Castro Manzano, J. Duarte Campderros, M. Fernandez, J. Garcia-Ferrero, G. Gomez, A. Graziano, A. Lopez Virto, J. Marco, R. Marco, C. Martinez Rivero, F. Matorras, F.J. Munoz Sanchez, J. Piedra Gomez, T. Rodrigo, A.Y. Rodríguez-Marrero, A. Ruiz-Jimeno, L. Scodellaro, I. Vila, R. Vilar Cortabitarte

CERN, European Organization for Nuclear Research, Geneva, Switzerland

D. Abbaneo, E. Auffray, G. Auzinger, M. Bachtis, P. Baillon, A.H. Ball, D. Barney, A. Benaglia, J. Bendavid, L. Benhabib, J.F. Benitez, G.M. Berruti, P. Bloch, A. Bocci, A. Bonato, C. Botta, H. Breuker, T. Camporesi, G. Cerminara, S. Colafranceschi³⁸, M. D'Alfonso, D. d'Enterria, A. Dabrowski, V. Daponte, A. David, M. De Gruttola, F. De Guio, A. De Roeck, S. De Visscher, E. Di Marco, M. Dobson, M. Dordevic, B. Dorney, T. du Pree, N. Dupont, A. Elliott-Peisert, G. Franzoni, W. Funk, D. Gigi, K. Gill, D. Giordano, M. Girone, F. Glege, R. Guida, S. Gundacker, M. Guthoff, J. Hammer, P. Harris, J. Hegeman, V. Innocente, P. Janot, H. Kirschenmann, M.J. Kortelainen, K. Kousouris, K. Krajczar, P. Lecoq, C. Lourenço, M.T. Lucchini, N. Magini, L. Malgeri, M. Mannelli, A. Martelli, L. Masetti, F. Meijers, S. Mersi, E. Meschi, F. Moortgat, S. Morovic, M. Mulders, M.V. Nemallapudi, H. Neugebauer, S. Orfanelli³⁹, L. Orsini, L. Pape, E. Perez, A. Petrilli, G. Petrucciani, A. Pfeiffer, D. Piparo, A. Racz, G. Rolandi⁴⁰, M. Rovere, M. Ruan, H. Sakulin, C. Schäfer, C. Schwick, A. Sharma, P. Silva, M. Simon, P. Sphicas⁴¹, D. Spiga, J. Steggemann, B. Stieger, M. Stoye, Y. Takahashi, D. Treille, A. Triossi, A. Tsirou, G.I. Veres¹⁹, N. Wardle, H.K. Wöhri, A. Zagodzinska⁴², W.D. Zeuner

Paul Scherrer Institut, Villigen, Switzerland

W. Bertl, K. Deiters, W. Erdmann, R. Horisberger, Q. Ingram, H.C. Kaestli, D. Kotlinski, U. Langenegger, D. Renker, T. Rohe

Institute for Particle Physics, ETH Zurich, Zurich, Switzerland

F. Bachmair, L. Bäni, L. Bianchini, M.A. Buchmann, B. Casal, G. Dissertori, M. Dittmar, M. Donegà, M. Dünser, P. Eller, C. Grab, C. Heidegger, D. Hits, J. Hoss, G. Kasieczka, W. Lustermann, B. Mangano, A.C. Marini, M. Marionneau, P. Martinez Ruiz del Arbol, M. Masciovecchio, D. Meister, P. Musella, F. Nessi-Tedaldi, F. Pandolfi, J. Pata, F. Pauss, L. Perrozzi, M. Peruzzi, M. Quittnat, M. Rossini, A. Starodumov⁴³, M. Takahashi, V.R. Tavolaro, K. Theofilatos, R. Wallny

Universität Zürich, Zurich, Switzerland

T.K. Aarrestad, C. AMSler⁴⁴, L. Caminada, M.F. Canelli, V. Chiochia, A. De Cosa, C. Galloni, A. Hinzmann, T. Hreus, B. Kilminster, C. Lange, J. Ngadiuba, D. Pinna, P. Robmann, F.J. Ronga, D. Salerno, Y. Yang

National Central University, Chung-Li, Taiwan

M. Cardaci, K.H. Chen, T.H. Doan, Sh. Jain, R. Khurana, M. Konyushikhin, C.M. Kuo, W. Lin, Y.J. Lu, R. Volpe, S.S. Yu

National Taiwan University (NTU), Taipei, Taiwan

R. Bartek, P. Chang, Y.H. Chang, Y.W. Chang, Y. Chao, K.F. Chen, P.H. Chen, C. Dietz, F. Fiori, U. Grundler, W.-S. Hou, Y. Hsiung, Y.F. Liu, R.-S. Lu, M. Miñano Moya, E. Petrakou, J.F. Tsai, Y.M. Tzeng

Chulalongkorn University, Faculty of Science, Department of Physics, Bangkok, Thailand

B. Asavapibhop, K. Kovitanggoon, G. Singh, N. Srimanobhas, N. Suwonjandee

Cukurova University, Adana, Turkey

A. Adiguzel, M.N. Bakirci⁴⁵, Z.S. Demiroglu, C. Dozen, I. Dumanoglu, E. Eskut, S. Girgis, G. Gokbulut, Y. Guler, E. Gurpinar, I. Hos, E.E. Kangal⁴⁶, A. Kayis Topaksu, G. Onengut⁴⁷, K. Ozdemir⁴⁸, A. Polatoz, D. Sunar Cerci⁴⁹, M. Vergili, C. Zorbilmez

Middle East Technical University, Physics Department, Ankara, Turkey

I.V. Akin, B. Bilin, S. Bilmis, B. Isildak⁵⁰, G. Karapinar⁵¹, U.E. Surat, M. Yalvac, M. Zeyrek

Bogazici University, Istanbul, Turkey

E.A. Albayrak⁵², E. Gülmez, M. Kaya⁵³, O. Kaya⁵⁴, T. Yetkin⁵⁵

Istanbul Technical University, Istanbul, Turkey

K. Cankocak, S. Sen⁵⁶, F.I. Vardarli

Institute for Scintillation Materials of National Academy of Science of Ukraine, Kharkov, Ukraine

B. Grynyov

National Scientific Center, Kharkov Institute of Physics and Technology, Kharkov, Ukraine

L. Levchuk, P. Sorokin

University of Bristol, Bristol, United Kingdom

R. Aggleton, F. Ball, L. Beck, J.J. Brooke, E. Clement, D. Cussans, H. Flacher, J. Goldstein, M. Grimes, G.P. Heath, H.F. Heath, J. Jacob, L. Kreczko, C. Lucas, Z. Meng, D.M. Newbold⁵⁷, S. Paramesvaran, A. Poll, T. Sakuma, S. Seif El Nasr-storey, S. Senkin, D. Smith, V.J. Smith

Rutherford Appleton Laboratory, Didcot, United Kingdom

K.W. Bell, A. Belyaev⁵⁸, C. Brew, R.M. Brown, D.J.A. Cockerill, J.A. Coughlan, K. Harder, S. Harper, E. Olaiya, D. Petyt, C.H. Shepherd-Themistocleous, A. Thea, L. Thomas, I.R. Tomalin, T. Williams, W.J. Womersley, S.D. Worm

Imperial College, London, United Kingdom

M. Baber, R. Bainbridge, O. Buchmuller, A. Bundock, D. Burton, S. Casasso, M. Citron, D. Colling, L. Corpe, N. Cripps, P. Dauncey, G. Davies, A. De Wit, M. Della Negra, P. Dunne, A. Elwood, W. Ferguson, J. Fulcher, D. Futyan, G. Hall, G. Iles, M. Kenzie, R. Lane, R. Lucas⁵⁷, L. Lyons, A.-M. Magnan, S. Malik, J. Nash, A. Nikitenko⁴³, J. Pela, M. Pesaresi, K. Petridis, D.M. Raymond, A. Richards, A. Rose, C. Seez, A. Tapper, K. Uchida, M. Vazquez Acosta⁵⁹, T. Virdee, S.C. Zenz

Brunel University, Uxbridge, United Kingdom

J.E. Cole, P.R. Hobson, A. Khan, P. Kyberd, D. Leggat, D. Leslie, I.D. Reid, P. Symonds, L. Teodorescu, M. Turner

Baylor University, Waco, USA

A. Borzou, K. Call, J. Dittmann, K. Hatakeyama, A. Kasmi, H. Liu, N. Pastika

The University of Alabama, Tuscaloosa, USA

O. Charaf, S.I. Cooper, C. Henderson, P. Rumerio

Boston University, Boston, USA

A. Avetisyan, T. Bose, C. Fantasia, D. Gastler, P. Lawson, D. Rankin, C. Richardson, J. Rohlf, J. St. John, L. Sulak, D. Zou

Brown University, Providence, USA

J. Alimena, E. Berry, S. Bhattacharya, D. Cutts, N. Dhingra, A. Ferapontov, A. Garabedian, U. Heintz, E. Laird, G. Landsberg, Z. Mao, M. Narain, S. Piperov, S. Sagir, T. Sinthuprasith, R. Syarif

University of California, Davis, Davis, USA

R. Breedon, G. Breto, M. Calderon De La Barca Sanchez, S. Chauhan, M. Chertok, J. Conway, R. Conway, P.T. Cox, R. Erbacher, M. Gardner, W. Ko, R. Lander, M. Mulhearn, D. Pellett, J. Pilot, F. Ricci-Tam, S. Shalhout, J. Smith, M. Squires, D. Stolp, M. Tripathi, S. Wilbur, R. Yohay

University of California, Los Angeles, USA

R. Cousins, P. Everaerts, C. Farrell, J. Hauser, M. Ignatenko, D. Saltzberg, E. Takasugi, V. Valuev, M. Weber

University of California, Riverside, Riverside, USA

K. Burt, R. Clare, J. Ellison, J.W. Gary, G. Hanson, J. Heilman, M. Ivova PANEVA, P. Jandir, E. Kennedy, F. Lacroix, O.R. Long, A. Luthra, M. Malberti, M. Olmedo Negrete, A. Shrinivas, H. Wei, S. Wimpenny

University of California, San Diego, La Jolla, USA

J.G. Branson, G.B. Cerati, S. Cittolin, R.T. D'Agnolo, A. Holzner, R. Kelley, D. Klein, J. Letts, I. Macneill, D. Olivito, S. Padhi, M. Pieri, M. Sani, V. Sharma, S. Simon, M. Tadel, A. Vartak, S. Wasserbaech⁶⁰, C. Welke, F. Würthwein, A. Yagil, G. Zevi Della Porta

University of California, Santa Barbara, Santa Barbara, USA

D. Barge, J. Bradmiller-Feld, C. Campagnari, A. Dishaw, V. Dutta, K. Flowers, M. Franco Sevilla, P. Geffert, C. George, F. Golf, L. Gouskos, J. Gran, J. Incandela, C. Justus, N. Mccoll, S.D. Mullin, J. Richman, D. Stuart, I. Suarez, W. To, C. West, J. Yoo

California Institute of Technology, Pasadena, USA

D. Anderson, A. Apresyan, A. Bornheim, J. Bunn, Y. Chen, J. Duarte, A. Mott, H.B. Newman, C. Pena, M. Pierini, M. Spiropulu, J.R. Vlimant, S. Xie, R.Y. Zhu

Carnegie Mellon University, Pittsburgh, USA

V. Azzolini, A. Calamba, B. Carlson, T. Ferguson, M. Paulini, J. Russ, M. Sun, H. Vogel, I. Vorobiev

University of Colorado Boulder, Boulder, USA

J.P. Cumalat, W.T. Ford, A. Gaz, F. Jensen, A. Johnson, M. Krohn, T. Mulholland, U. Nauenberg, K. Stenson, S.R. Wagner

Cornell University, Ithaca, USA

J. Alexander, A. Chatterjee, J. Chaves, J. Chu, S. Dittmer, N. Eggert, N. Mirman, G. Nicolas Kaufman, J.R. Patterson, A. Rinkevicius, A. Ryd, L. Skinnari, L. Soffi, W. Sun, S.M. Tan, W.D. Teo, J. Thom, J. Thompson, J. Tucker, Y. Weng, P. Wittich

Fermi National Accelerator Laboratory, Batavia, USA

S. Abdullin, M. Albrow, J. Anderson, G. Apollinari, L.A.T. Bauerdick, A. Beretvas, J. Berryhill, P.C. Bhat, G. Bolla, K. Burkett, J.N. Butler, H.W.K. Cheung, F. Chlebana, S. Cihangir, V.D. Elvira, I. Fisk, J. Freeman, E. Gottschalk, L. Gray, D. Green, S. Grünendahl, O. Gutsche, J. Hanlon, D. Hare, R.M. Harris, J. Hirschauer, B. Hooberman, Z. Hu, S. Jindariani, M. Johnson, U. Joshi,

A.W. Jung, B. Klima, B. Kreis, S. Kwan[†], S. Lammel, J. Linacre, D. Lincoln, R. Lipton, T. Liu, R. Lopes De Sá, J. Lykken, K. Maeshima, J.M. Marraffino, V.I. Martinez Outschoorn, S. Maruyama, D. Mason, P. McBride, P. Merkel, K. Mishra, S. Mrenna, S. Nahn, C. Newman-Holmes, V. O'Dell, K. Pedro, O. Prokofyev, G. Rakness, E. Sexton-Kennedy, A. Soha, W.J. Spalding, L. Spiegel, L. Taylor, S. Tkaczyk, N.V. Tran, L. Uplegger, E.W. Vaandering, C. Vernieri, M. Verzocchi, R. Vidal, H.A. Weber, A. Whitbeck, F. Yang, H. Yin

University of Florida, Gainesville, USA

D. Acosta, P. Avery, P. Bortignon, D. Bourilkov, A. Carnes, M. Carver, D. Curry, S. Das, G.P. Di Giovanni, R.D. Field, M. Fisher, I.K. Furic, J. Hugon, J. Konigsberg, A. Korytov, J.F. Low, P. Ma, K. Matchev, H. Mei, P. Milenovic⁶¹, G. Mitselmakher, L. Muniz, D. Rank, R. Rossin, L. Shchutska, M. Snowball, D. Sperka, J. Wang, S. Wang, J. Yelton

Florida International University, Miami, USA

S. Hewamanage, S. Linn, P. Markowitz, G. Martinez, J.L. Rodriguez

Florida State University, Tallahassee, USA

A. Ackert, J.R. Adams, T. Adams, A. Askew, J. Bochenek, B. Diamond, J. Haas, S. Hagopian, V. Hagopian, K.F. Johnson, A. Khatiwada, H. Prosper, V. Veeraraghavan, M. Weinberg

Florida Institute of Technology, Melbourne, USA

V. Bhopatkar, M. Hohlmann, H. Kalakhety, D. Mareskas-palcek, T. Roy, F. Yumiceva

University of Illinois at Chicago (UIC), Chicago, USA

M.R. Adams, L. Apanasevich, D. Berry, R.R. Betts, I. Bucinskaite, R. Cavanaugh, O. Evdokimov, L. Gauthier, C.E. Gerber, D.J. Hofman, P. Kurt, C. O'Brien, I.D. Sandoval Gonzalez, C. Silkworth, P. Turner, N. Varelas, Z. Wu, M. Zakaria

The University of Iowa, Iowa City, USA

B. Bilki⁶², W. Clarida, K. Dilsiz, S. Durgut, R.P. Gandrajula, M. Haytmyradov, V. Khristenko, J.-P. Merlo, H. Mermerkaya⁶³, A. Mestvirishvili, A. Moeller, J. Nachtman, H. Ogul, Y. Onel, F. Ozok⁵², A. Penzo, C. Snyder, P. Tan, E. Tiras, J. Wetzel, K. Yi

Johns Hopkins University, Baltimore, USA

I. Anderson, B.A. Barnett, B. Blumenfeld, D. Fehling, L. Feng, A.V. Gritsan, P. Maksimovic, C. Martin, M. Osherson, M. Swartz, M. Xiao, Y. Xin, C. You

The University of Kansas, Lawrence, USA

P. Baringer, A. Bean, G. Benelli, C. Bruner, J. Gray, R.P. Kenny III, D. Majumder, M. Malek, M. Murray, D. Noonan, S. Sanders, R. Stringer, Q. Wang, J.S. Wood

Kansas State University, Manhattan, USA

I. Chakaberia, A. Ivanov, K. Kaadze, S. Khalil, M. Makouski, Y. Maravin, A. Mohammadi, L.K. Saini, N. Skhirtladze, I. Svintradze, S. Toda

Lawrence Livermore National Laboratory, Livermore, USA

D. Lange, F. Rebassoo, D. Wright

University of Maryland, College Park, USA

C. Anelli, A. Baden, O. Baron, A. Belloni, B. Calvert, S.C. Eno, C. Ferraioli, J.A. Gomez, N.J. Hadley, S. Jabeen, R.G. Kellogg, T. Kolberg, J. Kunkle, Y. Lu, A.C. Mignerey, Y.H. Shin, A. Skuja, M.B. Tonjes, S.C. Tonwar

Massachusetts Institute of Technology, Cambridge, USA

A. Apyan, R. Barbieri, A. Baty, K. Bierwagen, S. Brandt, W. Busza, I.A. Cali, Z. Demiragli, L. Di

Matteo, G. Gomez Ceballos, M. Goncharov, D. Gulhan, Y. Iiyama, G.M. Innocenti, M. Klute, D. Kovalskyi, Y.S. Lai, Y.-J. Lee, A. Levin, P.D. Luckey, C. Mcginn, C. Mironov, X. Niu, C. Paus, D. Ralph, C. Roland, G. Roland, J. Salfeld-Nebgen, G.S.F. Stephans, K. Sumorok, M. Varma, D. Velicanu, J. Veverka, J. Wang, T.W. Wang, B. Wyslouch, M. Yang, V. Zhukova

University of Minnesota, Minneapolis, USA

B. Dahmes, A. Finkel, A. Gude, P. Hansen, S. Kalafut, S.C. Kao, K. Klapoetke, Y. Kubota, Z. Lesko, J. Mans, S. Nourbakhsh, N. Ruckstuhl, R. Rusack, N. Tambe, J. Turkewitz

University of Mississippi, Oxford, USA

J.G. Acosta, S. Oliveros

University of Nebraska-Lincoln, Lincoln, USA

E. Avdeeva, K. Bloom, S. Bose, D.R. Claes, A. Dominguez, C. Fangmeier, R. Gonzalez Suarez, R. Kamalieddin, J. Keller, D. Knowlton, I. Kravchenko, J. Lazo-Flores, F. Meier, J. Monroy, F. Ratnikov, J.E. Siado, G.R. Snow

State University of New York at Buffalo, Buffalo, USA

M. Alyari, J. Dolen, J. George, A. Godshalk, I. Iashvili, J. Kaisen, A. Kharchilava, A. Kumar, S. Rappoccio

Northeastern University, Boston, USA

G. Alverson, E. Barberis, D. Baumgartel, M. Chasco, A. Hortiangtham, B. Knapp, A. Massironi, D.M. Morse, D. Nash, T. Orimoto, R. Teixeira De Lima, D. Trocino, R.-J. Wang, D. Wood, J. Zhang

Northwestern University, Evanston, USA

K.A. Hahn, A. Kubik, N. Mucia, N. Odell, B. Pollack, A. Pozdnyakov, M. Schmitt, S. Stoynev, K. Sung, M. Trovato, M. Velasco

University of Notre Dame, Notre Dame, USA

A. Brinkerhoff, N. Dev, M. Hildreth, C. Jessop, D.J. Karmgard, N. Kellams, K. Lannon, S. Lynch, N. Marinelli, F. Meng, C. Mueller, Y. Musienko³³, T. Pearson, M. Planer, A. Reinsvold, R. Ruchti, G. Smith, S. Taroni, N. Valls, M. Wayne, M. Wolf, A. Woodard

The Ohio State University, Columbus, USA

L. Antonelli, J. Brinson, B. Bylsma, L.S. Durkin, S. Flowers, A. Hart, C. Hill, R. Hughes, K. Kotov, T.Y. Ling, B. Liu, W. Luo, D. Puigh, M. Rodenburg, B.L. Winer, H.W. Wulsin

Princeton University, Princeton, USA

O. Driga, P. Elmer, J. Hardenbrook, P. Hebda, S.A. Koay, P. Lujan, D. Marlow, T. Medvedeva, M. Mooney, J. Olsen, C. Palmer, P. Piroué, X. Quan, H. Saka, D. Stickland, C. Tully, J.S. Werner, A. Zuranski

University of Puerto Rico, Mayaguez, USA

S. Malik

Purdue University, West Lafayette, USA

V.E. Barnes, D. Benedetti, D. Bortoletto, L. Gutay, M.K. Jha, M. Jones, K. Jung, M. Kress, D.H. Miller, N. Neumeister, F. Primavera, B.C. Radburn-Smith, X. Shi, I. Shipsey, D. Silvers, J. Sun, A. Svyatkovskiy, F. Wang, W. Xie, L. Xu, J. Zablocki

Purdue University Calumet, Hammond, USA

N. Parashar, J. Stupak

Rice University, Houston, USA

A. Adair, B. Akgun, Z. Chen, K.M. Ecklund, F.J.M. Geurts, M. Guilbaud, W. Li, B. Michlin, M. Northup, B.P. Padley, R. Redjimi, J. Roberts, J. Rorie, Z. Tu, J. Zabel

University of Rochester, Rochester, USA

B. Betchart, A. Bodek, P. de Barbaro, R. Demina, Y. Eshaq, T. Ferbel, M. Galanti, A. Garcia-Bellido, P. Goldenzweig, J. Han, A. Harel, O. Hindrichs, A. Khukhunaishvili, G. Petrillo, M. Verzetti

The Rockefeller University, New York, USA

L. Demortier

Rutgers, The State University of New Jersey, Piscataway, USA

S. Arora, A. Barker, J.P. Chou, C. Contreras-Campana, E. Contreras-Campana, D. Duggan, D. Ferencek, Y. Gershtein, R. Gray, E. Halkiadakis, D. Hidas, E. Hughes, S. Kaplan, R. Kunnawalkam Elayavalli, A. Lath, K. Nash, S. Panwalkar, M. Park, S. Salur, S. Schnetzer, D. Sheffield, S. Somalwar, R. Stone, S. Thomas, P. Thomassen, M. Walker

University of Tennessee, Knoxville, USA

M. Foerster, G. Riley, K. Rose, S. Spanier, A. York

Texas A&M University, College Station, USA

O. Bouhali⁶⁴, A. Castaneda Hernandez, M. Dalchenko, M. De Mattia, A. Delgado, S. Dildick, R. Eusebi, W. Flanagan, J. Gilmore, T. Kamon⁶⁵, V. Krutelyov, R. Montalvo, R. Mueller, I. Osipenkov, Y. Pakhotin, R. Patel, A. Perloff, J. Roe, A. Rose, A. Safonov, A. Tatarinov, K.A. Ulmer²

Texas Tech University, Lubbock, USA

N. Akchurin, C. Cowden, J. Damgov, C. Dragoiu, P.R. Duerdo, J. Faulkner, S. Kunori, K. Lamichhane, S.W. Lee, T. Libeiro, S. Undleeb, I. Volobouev

Vanderbilt University, Nashville, USA

E. Appelt, A.G. Delannoy, S. Greene, A. Gurrola, R. Janjam, W. Johns, C. Maguire, Y. Mao, A. Melo, H. Ni, P. Sheldon, B. Snook, S. Tuo, J. Velkovska, Q. Xu

University of Virginia, Charlottesville, USA

M.W. Arenton, S. Boutle, B. Cox, B. Francis, J. Goodell, R. Hirosky, A. Ledovskoy, H. Li, C. Lin, C. Neu, E. Wolfe, J. Wood, F. Xia

Wayne State University, Detroit, USA

C. Clarke, R. Harr, P.E. Karchin, C. Kottachchi Kankanamge Don, P. Lamichhane, J. Sturdy

University of Wisconsin, Madison, USA

D.A. Belknap, D. Carlsmith, M. Cepeda, A. Christian, S. Dasu, L. Dodd, S. Duric, E. Friis, B. Gomber, R. Hall-Wilton, M. Herndon, A. Hervé, P. Klabbers, A. Lanaro, A. Levine, K. Long, R. Loveless, A. Mohapatra, I. Ojalvo, T. Perry, G.A. Pierro, G. Polese, I. Ross, T. Ruggles, T. Sarangi, A. Savin, A. Sharma, N. Smith, W.H. Smith, D. Taylor, N. Woods

†: Deceased

1: Also at Vienna University of Technology, Vienna, Austria

2: Also at CERN, European Organization for Nuclear Research, Geneva, Switzerland

3: Also at State Key Laboratory of Nuclear Physics and Technology, Peking University, Beijing, China

4: Also at Institut Pluridisciplinaire Hubert Curien, Université de Strasbourg, Université de Haute Alsace Mulhouse, CNRS/IN2P3, Strasbourg, France

-
- 5: Also at National Institute of Chemical Physics and Biophysics, Tallinn, Estonia
 - 6: Also at Skobeltsyn Institute of Nuclear Physics, Lomonosov Moscow State University, Moscow, Russia
 - 7: Also at Universidade Estadual de Campinas, Campinas, Brazil
 - 8: Also at Centre National de la Recherche Scientifique (CNRS) - IN2P3, Paris, France
 - 9: Also at Laboratoire Leprince-Ringuet, Ecole Polytechnique, IN2P3-CNRS, Palaiseau, France
 - 10: Also at Joint Institute for Nuclear Research, Dubna, Russia
 - 11: Also at Zewail City of Science and Technology, Zewail, Egypt
 - 12: Now at Helwan University, Cairo, Egypt
 - 13: Also at Ain Shams University, Cairo, Egypt
 - 14: Now at British University in Egypt, Cairo, Egypt
 - 15: Also at Université de Haute Alsace, Mulhouse, France
 - 16: Also at Tbilisi State University, Tbilisi, Georgia
 - 17: Also at Brandenburg University of Technology, Cottbus, Germany
 - 18: Also at Institute of Nuclear Research ATOMKI, Debrecen, Hungary
 - 19: Also at Eötvös Loránd University, Budapest, Hungary
 - 20: Also at University of Debrecen, Debrecen, Hungary
 - 21: Also at Wigner Research Centre for Physics, Budapest, Hungary
 - 22: Also at University of Visva-Bharati, Santiniketan, India
 - 23: Now at King Abdulaziz University, Jeddah, Saudi Arabia
 - 24: Also at University of Ruhuna, Matara, Sri Lanka
 - 25: Also at Isfahan University of Technology, Isfahan, Iran
 - 26: Also at University of Tehran, Department of Engineering Science, Tehran, Iran
 - 27: Also at Plasma Physics Research Center, Science and Research Branch, Islamic Azad University, Tehran, Iran
 - 28: Also at Università degli Studi di Siena, Siena, Italy
 - 29: Also at Purdue University, West Lafayette, USA
 - 30: Also at International Islamic University of Malaysia, Kuala Lumpur, Malaysia
 - 31: Also at Malaysian Nuclear Agency, MOSTI, Kajang, Malaysia
 - 32: Also at Consejo Nacional de Ciencia y Tecnología, Mexico city, Mexico
 - 33: Also at Institute for Nuclear Research, Moscow, Russia
 - 34: Also at St. Petersburg State Polytechnical University, St. Petersburg, Russia
 - 35: Also at National Research Nuclear University 'Moscow Engineering Physics Institute' (MEPhI), Moscow, Russia
 - 36: Also at California Institute of Technology, Pasadena, USA
 - 37: Also at Faculty of Physics, University of Belgrade, Belgrade, Serbia
 - 38: Also at Facoltà Ingegneria, Università di Roma, Roma, Italy
 - 39: Also at National Technical University of Athens, Athens, Greece
 - 40: Also at Scuola Normale e Sezione dell'INFN, Pisa, Italy
 - 41: Also at University of Athens, Athens, Greece
 - 42: Also at Warsaw University of Technology, Institute of Electronic Systems, Warsaw, Poland
 - 43: Also at Institute for Theoretical and Experimental Physics, Moscow, Russia
 - 44: Also at Albert Einstein Center for Fundamental Physics, Bern, Switzerland
 - 45: Also at Gaziosmanpasa University, Tokat, Turkey
 - 46: Also at Mersin University, Mersin, Turkey
 - 47: Also at Cag University, Mersin, Turkey
 - 48: Also at Piri Reis University, Istanbul, Turkey
 - 49: Also at Adiyaman University, Adiyaman, Turkey
 - 50: Also at Ozyegin University, Istanbul, Turkey

- 51: Also at Izmir Institute of Technology, Izmir, Turkey
- 52: Also at Mimar Sinan University, Istanbul, Istanbul, Turkey
- 53: Also at Marmara University, Istanbul, Turkey
- 54: Also at Kafkas University, Kars, Turkey
- 55: Also at Yildiz Technical University, Istanbul, Turkey
- 56: Also at Hacettepe University, Ankara, Turkey
- 57: Also at Rutherford Appleton Laboratory, Didcot, United Kingdom
- 58: Also at School of Physics and Astronomy, University of Southampton, Southampton, United Kingdom
- 59: Also at Instituto de Astrofísica de Canarias, La Laguna, Spain
- 60: Also at Utah Valley University, Orem, USA
- 61: Also at University of Belgrade, Faculty of Physics and Vinca Institute of Nuclear Sciences, Belgrade, Serbia
- 62: Also at Argonne National Laboratory, Argonne, USA
- 63: Also at Erzincan University, Erzincan, Turkey
- 64: Also at Texas A&M University at Qatar, Doha, Qatar
- 65: Also at Kyungpook National University, Daegu, Korea